

General Disclaimer

One or more of the Following Statements may affect this Document

- This document has been reproduced from the best copy furnished by the organizational source. It is being released in the interest of making available as much information as possible.
- This document may contain data, which exceeds the sheet parameters. It was furnished in this condition by the organizational source and is the best copy available.
- This document may contain tone-on-tone or color graphs, charts and/or pictures, which have been reproduced in black and white.
- This document is paginated as submitted by the original source.
- Portions of this document are not fully legible due to the historical nature of some of the material. However, it is the best reproduction available from the original submission.

TEXAS A&M UNIVERSITY

THE DESIGN, ANALYSIS AND EXPERIMENTAL
EVALUATION OF AN ELASTIC MODEL WING

by

Ralph K. Cavin, III and Chavalit Thisayakorn



DEPARTMENT OF ELECTRICAL ENGINEERING
College Station, Texas

(NASA-CR-144535) THE DESIGN, ANALYSIS AND
EXPERIMENTAL EVALUATION OF AN ELASTIC MODEL
WING (Texas A&M Univ.) 51 p HC \$4.25

N76-10092

CSCS 01C

Unclas
39397

G3/05

THE DESIGN, ANALYSIS AND EXPERIMENTAL
EVALUATION OF AN ELASTIC MODEL WING

by

Ralph K. Cavin, III and Chavalit Thisayakorn

NAS 9-11303

September 1974
Department of Electrical Engineering
Texas A&M University

TABLE OF CONTENTS

TITLE	PAGE
Table of Contents	ii
List of Tables	iii
List of Figures	iv
Section I Introduction	1
Section II Design and Fabrication of the Elastic Wing	2
Section III Design Calculations	5
A. The Structural Model	5
B. Aerodynamics Development	11
C. The Static Aeroelasticity Problem	16
D. Flutter Problem	17
Section IV Description of Tests	20
A. Static Tests	20
B. Wind Tunnel Tests	20
Section V Comparison of Analytical and Experimental Results	21
Section VI Discussion	26
References	30
Appendix A	31
Appendix B	44

LIST OF TABLES

TABLE	TITLE	PAGE
1	Spar Dimensions	6
2	Data on Steel Ribs of the Wing	10

LIST OF FIGURES:

FIGURE	TITLE	
1	Elastic Model Wing Planform	3
2	Rib-Air Foil	3
3	Cross-sectional Structural Description at the Model Wing Construction	4
4	Definition of Symbols for Beam Cross-section	7
5	Definition of Structural Node Displacements	7
6	Spanwise Slice of Wing Showing Definition of Symbols	13
7	Definition of Positive Sense for Displacements at Node j	13
8	Comparison of the Static Load Test Linear Deflections	22
9	Comparison of the Static Load Twist Angle	22
10	Plots of Vertical Deflections Measured in the Wind Tunnel	23
11	Lift Coefficient C_L versus Angle of Attack α	24
12	Plots of the Twist Angles Measured from the Wind Tunnel	25
13	Comparison of the Elastic Deflections	27
14	Comparison of Twist Angles	28

THE DESIGN, ANALYSIS, AND EXPERIMENTAL
EVALUATION OF AN ELASTIC MODEL WING

by

Ralph K. Cavin, III, and Chavalit Thisayakorn

(I) Introduction

It is common practice in preliminary static aeroelastic analyses to estimate elastic increments in stability derivatives by utilizing a clamped-vehicle stiffness matrix in conjunction with an aerodynamic influence matrix determined for the configuration by use of the linear, inviscid aerodynamic theory. These aeroelastic estimates are normally refined by 'freeing' the structure and including vehicle mass effects based upon the use of mean axis vehicle coordinate systems. [1] The computer program FLEXSTAB, which was written by The Boeing Airplane Company under the sponsorship of NASA-AMES, is a relatively sophisticated implementation of these basic ideas. FLEXSTAB has the capability of admitting two different types of structural representations. If the structural characteristics of the vehicle are adequately represented by the interconnection of beam elements, then FLEXSTAB accepts the beam EI and GK characteristics and generates the required structural matrices. On the other hand, the structural matrices can be generated externally in a finite element program, without the restriction of beam-like structural properties, and the results can be entered directly into FLEXSTAB.

The primary objective of this study was to develop experimental data from a carefully controlled elastic model to be used in evaluating the effectiveness of aeroelasticity programs such as FLEXSTAB for vehicles of the orbiter class. In order to accomplish this objective at a minimum cost it was decided to utilize an existing rigid 5% fuselage model for the 002 Orbiter configuration,

and to construct elastic wings for the model. The 002 Orbiter wings were straight with moderate aspect ratio and were therefore amenable to a beam-like structural representation.

(II) Design and Fabrication of the Elastic Wing

In view of the assumed beam-like structure of the 002 Orbiter wing, it was decided that the load carrying member of the model wing should be a beam with well defined EI and GK characteristics. It was further decided that the distribution of EI and GK along the wing span should parallel the 002 EI and GK shapes provided to A&M by the NASA-JSC Structures group. However, no attempt was made to scale the given (Stiff) beam characteristics to the 5% model. Rather the selection of EI and GK was based upon the criterion that measurable deformations and stability derivative changes should occur under expected aerodynamic load.

The basic design philosophy that evolved was that the aerodynamic loads should be transmitted to the beam via rib members. Further, in order to approximate the finite-element aerodynamic methods, the wing surface was segmented in a streamwise manner and each segment was rigidly attached to a corresponding rib element. Figure 1 is a planform view showing location of the Elastic Axis, as well as the basic aerodynamic sections for the wing. The NACA airfoil descriptions are given in Figure 2. As can be seen from Figure 1, the elastic axis is swept aft at an angle of 9.75 degrees from the vertical.

Figure 3 depicts the basic construction of the elastic wing. Note that each panel section is made of low density Balsa Wood which is cemented to the supporting rib member. The region between adjacent panel sections is approximately 1/16" wide and is filled with an ultra soft Neoprene gasket that

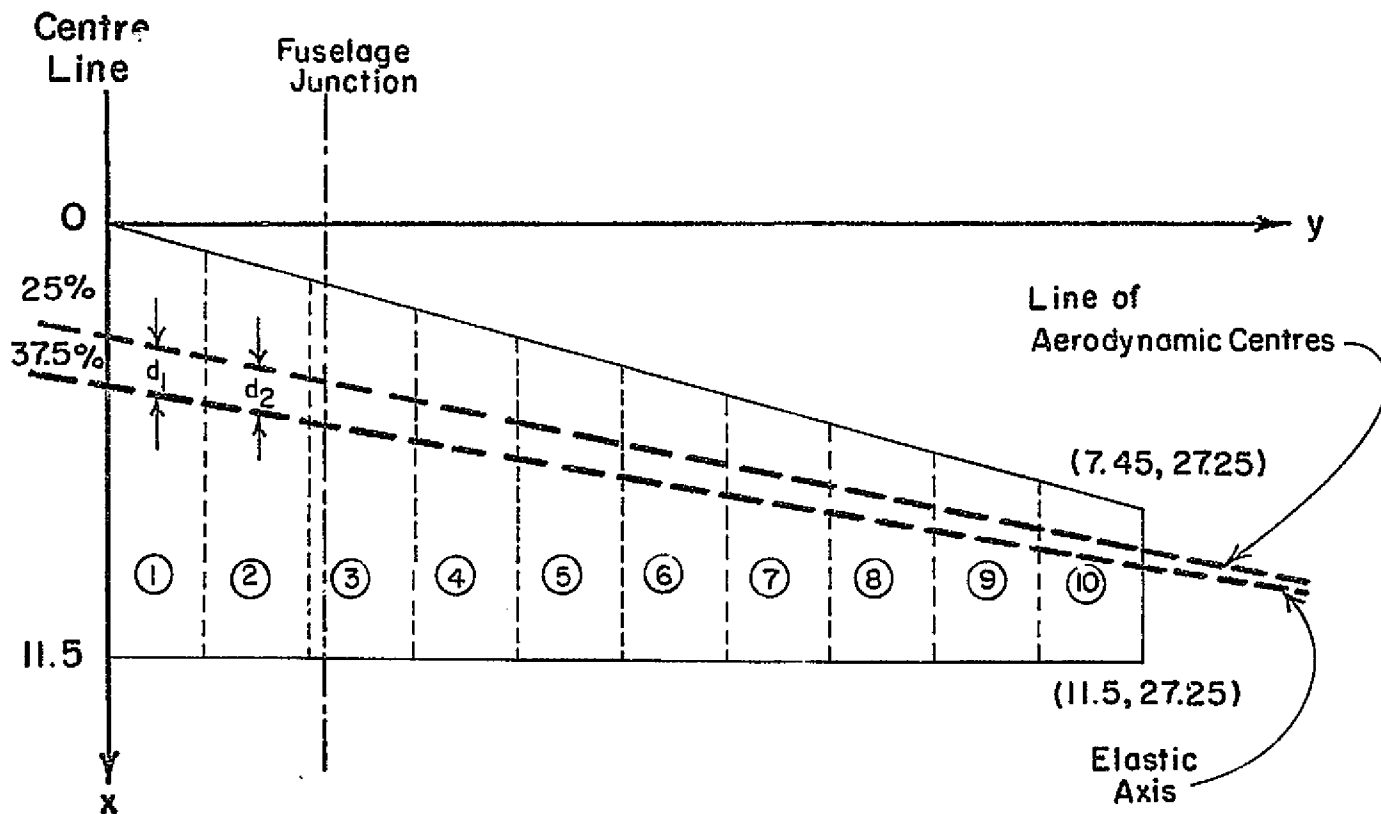


FIGURE 1. Elastic Model Wing Planform (5% 002 orbiter wing)

AIR-FOIL: ROOT NACA 0014
TIP NACA 0010

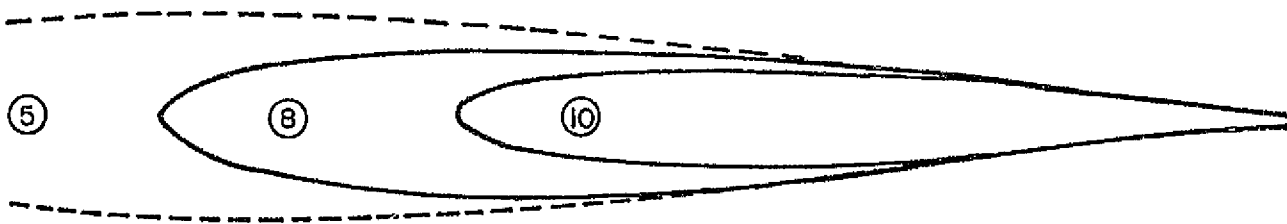


FIGURE 2. Rib-Airfoil (full size model wing cross-sections)

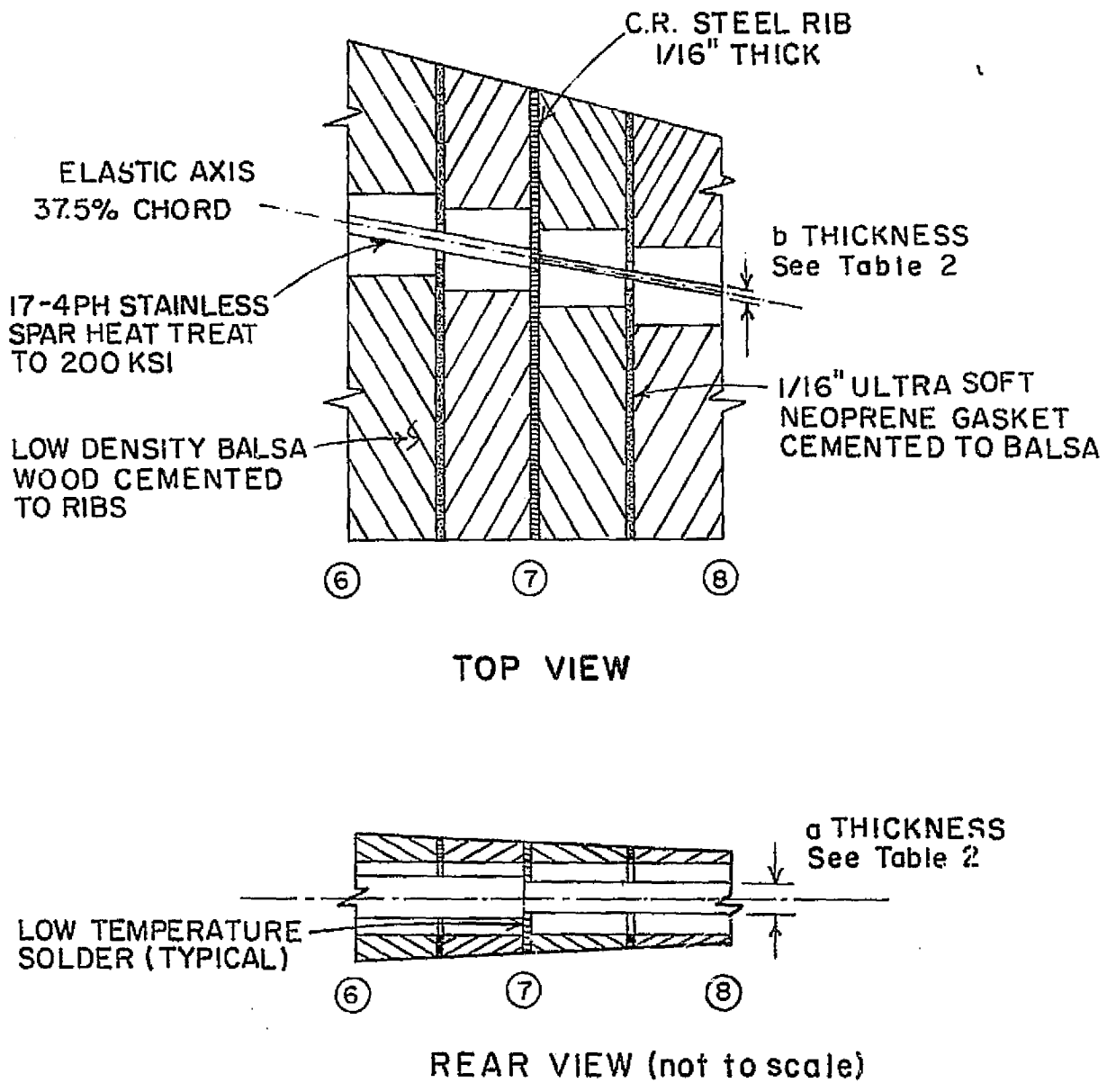


FIGURE 3. Cross-Sectional structural description at the Model-Wing Construction.

is cemented to the Balsa. Stress Calculations indicated that a high strength alloy of stainless steel could be used for the wing spar but that heat treatment was required after machining. This process allowed a 2.5 safety factor on ultimate strength and about 2.3 on yield strength. (No allowance was made for dynamic loads.) Ribs were made of the same material as the spar for ease of attachment. The spar was designed to have a rectangular cross section so that the rib elements could be firmly attached to the spar. Table 1 contains the dimensional data for the spar. The computed values for EI and GK are also listed in this table. The cross sectional moment data which was computed by using the formulae [4]

$$K = \frac{ba^3}{3} - \frac{64a^4}{\pi^5} \tanh\left(\frac{\pi b}{2a}\right) . \quad (1)$$

$$I_x = \int z^2 dA = \frac{ba^3}{12} \quad (2)$$

The above symbols are defined in Figure 4.

(III) Design Calculations

The purpose of this section is to describe the analysis methods that were utilized in the design of the elastic wing described in Section II. Two basic analytical tools were utilized in the evolution of structural specifications for the wing; namely the Doublet Lattice Aerodynamic lifting surface procedure and the finite element structural analysis method for beam members. In the following, we first discuss the analytical formulation for the general, time-dependent problem. After this broad notational framework has been established, the special static-aeroelastic and flutter problems are considered.

A. The Structural Model

As has already been pointed out, the principal load-carrying member in the wing structure is the spar element. The spar is essentially a beam element with

Spanwise Panel (location number)	b - Thickness (inches)	a - Thickness (inches)	Lengths (inches)
2-3	0.391	0.407	1.078
3-4	0.369	0.355	2.828
4-5	0.273	0.368	2.828
5-6	0.243	0.310	2.828
6-7	0.173	0.300	2.828
7-8	0.152	0.246	2.828
8-9	0.146	0.188	2.828
9-10	0.129	0.152	2.891

Table 1. Spar Dimensions (See also Figure 3)

Station Number of Spanwise Segments	Values of EI (lb - in ²)	Values of GK (lb - in ²)
3	63687.50	40090.40
4	39837.50	27166.72
5	32875.00	15314.09
6	17575.00	8730.85
7	11325.00	3718.85
8	5468.75	1990.35
9	2343.75	1156.62
10	1093.75	600.77

Table 1. (continued)

Values of EI and GK for wing spar

$$E = 2.9 \times 10^7 \text{ lb/in}^2$$

$$G = 1.12 \times 10^7 \text{ lb/in}^2$$

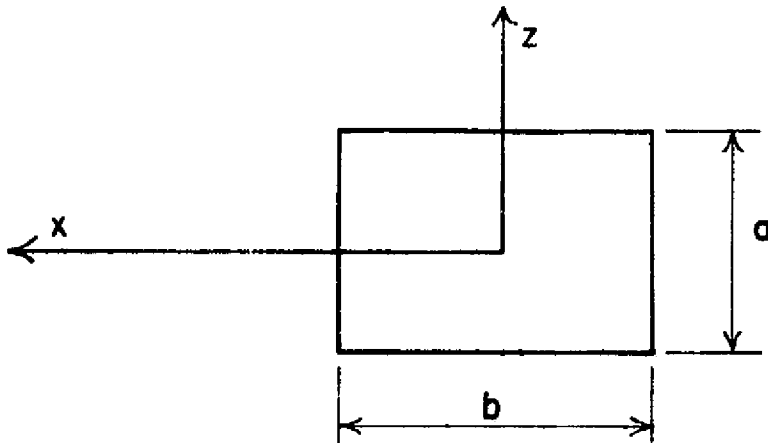


FIGURE 4. Definition of symbols for beam Cross - section.

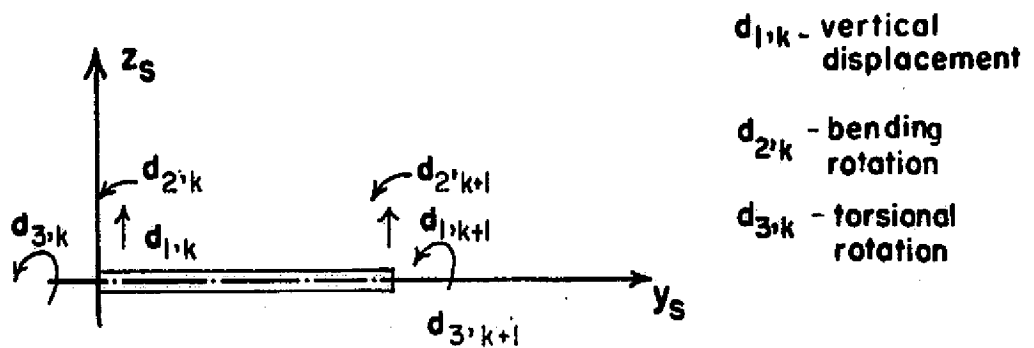


FIGURE 5. Definition of structural nodal displacements.

rectangular sections of length 2.8 in. whose sectional area progressively decreases in the spanwise direction. There are 8 spar sections, each with a possibility of 6 physical degrees of freedom per section, implying a maximum of 48 structural degrees of freedom. However, in view of the planned testing of the wing at very small (less than ten degrees) angles of attack, it was decided that in-plane bending of the spar would be minimal and hence only torsional and normal bending degrees of freedom were retained for each beam element. The degrees of freedom associated with each element are defined in Figure 5. The elemental stiffness matrix for the member shown in Figure 5 therefore reduces to [2].

$$\begin{array}{cccccc}
 & d_{1,K} & d_{2,K} & d_{3,K} & d_{1,K+1} & d_{2,K+1} & d_{3,K+1} \\
 [K]_x = & \left[\begin{array}{cccccc}
 12 EI_x / \ell^3, & & & & & & \\
 6 EI_x / \ell^2, & 4 EI_x / \ell, & & & & & \\
 0, & 0, & GK / \ell, & & & & \\
 -12 EI_x / \ell^3, & -6 EI_x / \ell^2, & 0, & 12 EI_x / \ell^3, & & & \\
 -6 EI_x / \ell^2, & 0, & 0, & -6 EI_x / \ell^2, & 4 EI_x / \ell, & & \\
 0, & 0, & GK / \ell, & 0, & 0, & GK / \ell, &
 \end{array} \right] & \text{symmetric} \\
 & & & & & & (3)
 \end{array}$$

A composite stiffness matrix can be generated by appropriately combining the element matrices in an underlying structural reference frame. In view of the fact that the spar is straight, the assembly task is quite straight-forward in this case and can be accomplished by overlaying successive element matrices and adding overlapping terms, e.g.,

Station number of ribs	Distances of ribs' c.g. off from the elastic axis (in.)	Rib mass (slug) x 10 ⁻³	Polar Mass moment of inertia (slug-in ²) x 10 ⁻²
3	0.706527	0.243999	0.140291
4	0.651691	0.201206	0.098401
5	0.596856	0.163412	0.067019
6	0.542019	0.130345	0.044076
7	0.487183	0.101735	0.027786
8	0.432345	0.077311	0.016626
9	0.377509	0.0568	0.009311
10	0.322672	0.039931	0.004781

Table 2. Data on steel ribs of the wing

Since the wing spar is swept at an angle, Λ , of 9.75 degrees, it is necessary to transform the spar structural matrices into a coordinate frame compatible with the aerodynamic frame. This is easily accomplished by performing the following transformation

$$[K]_1 = [T] [K] [T]^T$$

where $T =$

$$\begin{bmatrix} 1 & 0 & 0 & 0 & 0 & 0 \\ 0 & \cos \theta & -\sin \theta & 0 & 0 & 0 \\ 0 & \sin \theta & \cos \theta & 0 & 0 & 0 \\ 0 & 0 & 0 & 1 & 0 & 0 \\ 0 & 0 & 0 & 0 & \cos \theta & -\sin \theta \\ 0 & 0 & 0 & 0 & \sin \theta & \cos \theta \end{bmatrix}$$

B. Aerodynamics Development

The basic procedure that has been used to treat aerodynamic forces is based on the Doublet-Lattice-Method (D.L.M.) [3]. Fundamentally, the D.L.M. yields a set of Aerodynamic Influence Coefficients, $[D]$, relating the assumed harmonic motion of the normal wash, $\{w\}$, at specified points on the wing surface to the pressure differential, $\{\Delta C_p\}$, across the wing. Specifically, the integral equation

$$w(x,y,z) = \frac{1}{8\pi} \int \int_{\text{lifting surface}} K(x-\xi, y-\eta, z-\zeta; \omega, M) \Delta C_p \, d\xi \, d\sigma \quad (5)$$

is approximately solved as

$$\{w\} = [D] \{\Delta C_p\} \quad (6)$$

where the velocity normal to the oscillating surface is

$$\{W\} = U_\infty \operatorname{Re} [\{w\} e^{i\omega t}], \quad (7)$$

and the pressure differential is

$$\{\Delta p\} = q_\infty \operatorname{Re} [\{\Delta C_p\} e^{i\omega t}]. \quad (8)$$

Let us now consider specifically the computation of the aerodynamic forces for later use.

In general, l_{ij} is the distance from the j th. structural node to the 1/4 chord point for the ij th. panel and r_{ij} is the distance from the j th. structural node to the 3/4 chord point for the ij th. panel (See Figure 6). The total force acting on the ij th. panel is given by

$$f_{ij} = \Delta p_{ij} A_{ij} \quad (9)$$

and will be assumed to be acting at the center of the 3/4 chord point of the ij th. panel. In order to define the sense of the various forces and moments due to the aerodynamic forces, we must first define the assumed positive displacement at node j . This is done in Figure 7, the force tending to increase the d_1 coordinate is

$$f_{ij} = \sum_{i=1}^P \Delta p_{ij} A_{ij}, \quad (10)$$

the force tending to increase d_2 is zero and the force tending to increase d_3 is

$$f_{3j} = -\sum_{i=1}^P l_{ij} \Delta p_{ij} A_{ij}, \quad (\text{a moment}) \quad (11)$$

where we assume that l_{ij} and r_{ij} carry the sign of their x-coordinate location. We will further assume that there are Q spanwise panel rows and P chordwise panel rows, implying that n , the dimension of $\{d\}$ is $3Q$.

Let us now consider the computation of the normal wash W in terms of the displacements at the structural node points. By definition, the normal wash must be equal to the substantial derivative of the vertical displacement of the surface. (Implying no fluid flow through the surface.) In particular, we are interested in satisfying this boundary condition at the 3/4 chord points for each panel. The vertical displacement at any point along the chordwise centerline through node j is

$$z_j = d_{1j} - x d_{3j}, \quad (12)$$

where the definitions of Figure 7 have been used. The substantial derivative is therefore

$$W_j(t) = \frac{D(z_j)}{Dt} = \dot{d}_{1j} - x \dot{d}_{3j} - U_{\infty} d_{3j}. \quad (13)$$

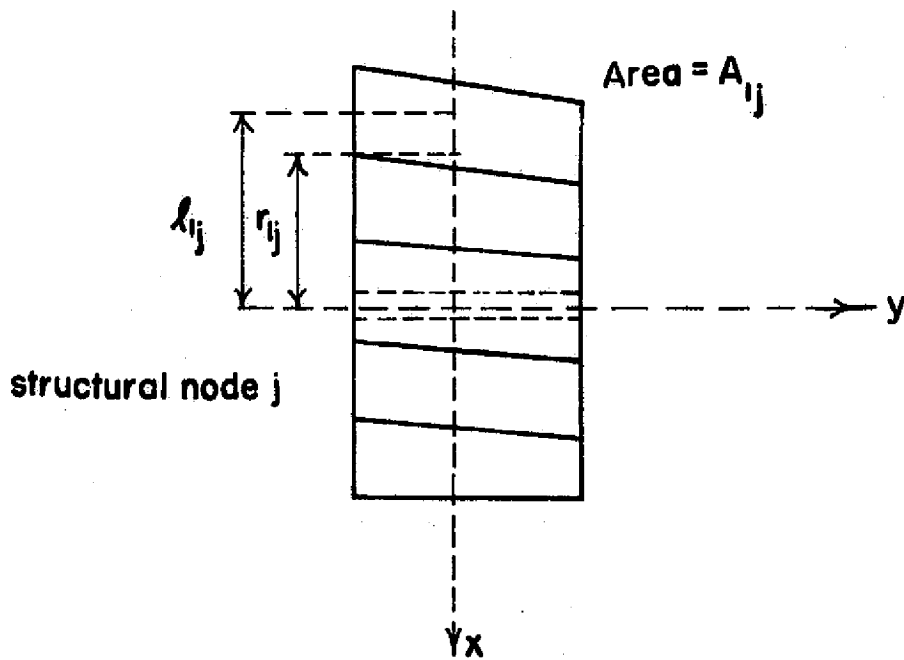


FIGURE 6. Span-wise slice of wing showing definition of symbols.



FIGURE 7. Definition of positive sense for displacements at node j .

Consequently, the downwash at the 3/4 chord of the ij th. panel can be written. (Assuming no chordwise deformation).

$$w_{ij}(t) = \overset{\circ}{d}_{ij} - r_{ij} \overset{\circ}{d}_{3j} - U_{\alpha} \overset{\circ}{d}_{3j}. \quad (14)$$

Further, if w_{ij} is assumed to be of exponential form,

$$w_{ij}(t) = w_{ij} e^{i\omega t},$$

(14) becomes

$$w_{ij} = d_{ij}(i\omega) - r_{ij} d_{3j}(i\omega) - U_{\alpha} d_{3j} \quad (15)$$

Let us now return to (6) and establish the mechanism for computing the generalized nodal forces. Denote

$$\{w\} = \{w_{11} \ w_{12} \ \dots \ w_{1Q} \mid w_{21} \ w_{22} \ \dots \ w_{2Q} \mid \dots \mid w_{P1} \ w_{P2} \ \dots \ w_{PQ}\}^T \quad (16)$$

In (6), $[D]$ is therefore a matrix of dimension $PQ \times PX$. Let the force vector $\{f\}$, the pressure vector, $\{\Delta p\}$, etc. be defined using the same ordering as (16).

In addition, let the generalized forces at node k be ordered as

$$\begin{aligned} f_{1k} &= \text{vertical deformation force} \\ f_{2k} &= \text{bending deformation moment} \\ f_{3k} &= \text{torsional deformation moment,} \end{aligned}$$

and define

$$\{f\}_s^T = \{f_{11} \ f_{21} \ f_{31} \mid f_{12} \ f_{22} \ f_{32} \mid \dots \mid f_{1Q} \ f_{2Q} \ f_{3Q}\}, \quad (17)$$

i.e., $\{f\}_s$ denotes the vector of forces acting at the structural nodes. We must now develop appropriate transformation matrices so that $\{f\}_s$ can be calculated in terms of nodal displacements $\{d\}$. From (10) and (11), we can write

$$\{f\}_s = \begin{matrix} 3Q & 3Q \times PQ & PQ \\ [G] & \{\Delta p\} \end{matrix} \quad (18)$$

$$[E] = \begin{matrix} \left. \begin{matrix} 1 & 0 & -r_{11} & 0 & 0 & 0 & \dots & 0 & 0 & 0 \\ 0 & 0 & 0 & 1 & 0 & -r_{12} & \dots & 0 & 0 & 0 \\ \dots & \dots & \dots & \dots & \dots & \dots & \dots & \dots & \dots & \dots \\ 0 & 0 & 0 & 0 & 0 & 0 & \dots & 1 & 0 & -r_{1Q} \\ 1 & 0 & -r_{21} & 0 & 0 & 0 & \dots & 0 & 0 & 0 \\ 0 & 0 & 0 & 1 & 0 & -r_{22} & \dots & 0 & 0 & 0 \\ \dots & \dots & \dots & \dots & \dots & \dots & \dots & \dots & \dots & \dots \\ 0 & 0 & 0 & 0 & 0 & 0 & \dots & 1 & 0 & -r_{2Q} \\ \dots & \dots & \dots & \dots & \dots & \dots & \dots & \dots & \dots & \dots \\ 1 & 0 & -r_{P1} & 0 & 0 & 0 & \dots & 0 & 0 & 0 \\ 0 & 0 & 0 & 1 & 0 & -r_{P2} & \dots & 0 & 0 & 0 \\ \dots & \dots & \dots & \dots & \dots & \dots & \dots & \dots & \dots & \dots \\ 0 & 0 & 0 & 0 & 0 & 0 & \dots & 1 & 0 & -r_{PQ} \end{matrix} \right\} & \left. \begin{matrix} \\ \end{matrix} \right\} \begin{matrix} Q \\ \\ \\ PQ \\ \\ \\ PQ \\ \\ \\ PQ \\ \\ \\ PQ \\ \\ \\ PQ \end{matrix} \end{matrix} \quad (23)$$

If we now combine (18), (20) and (21), we can finally write

$$\{f\}_s = \frac{q_\infty}{U_\infty} [G] [D(\omega)]^{-1} \{[H] + i\omega[E]\} \{d\} \quad (24)$$

C. The Static Aeroelasticity Problem

The bulk of the analytical work conducted during this study involved the estimation of elastic deformations under steady flow conditions. In this case, ω is set to zero in the aerodynamic matrices and D is defined over the field of real numbers. Hence (24) reduces to

$$\{f\}_s = \frac{q_\infty}{U_\infty} [G] [D]^{-1} [H] \{d\} \quad (25)$$

Gravitational loading of the wing was neglected because it was found that these forces were small compared to expected aerodynamic forces. The result of combining (25) with the composite stiffness matrix whose development was outlined in Section III-A is the following expression

$$[K] \{d\} = \frac{q_\infty}{U_\infty} [G] [D]^{-1} [H] (\{d\} + \alpha \{1\}) \quad (26)$$

where $\{1\}$ is a vector of length $3Q$ each of whose components is a one. In effect, the term in parentheses on the right hand side of (26) contains a term dependent upon the elastic deformation $\{d\}$ and a term dependent upon the rigid angle of attack, α . Now it is a simple matter to indicate the solution to (26), e.g.

$$\{d\} = ([K] - \frac{q_\infty}{U_\infty} [G] [D]^{-1} [H])^{-1} \frac{q_\infty}{U_\infty} [G] [D]^{-1} [H] \{1\} \alpha \quad (27)$$

A computer program was written to implement (27) using the planar doublet lattice procedure (vortex lattice for steady flow) to calculate the deformed wing shape under a specified Mach number, q_∞ and rigid angle of attack, α . All theoretical aeroelasticity results described in Section IV of this report, were obtained via this procedure. A listing for this computer program is given in Appendix A.

D. Flutter Problem

The basic problem in flutter analysis is that of determining if the wing will develop oscillatory motions under test conditions. This requires the inclusion of appropriate mass matrices and an unsteady aerodynamics capability into the existing computer code).

By utilization of matrix structural analysis methods, discrete mass and stiffness matrices have been developed for the wing under consideration (See Section III). The resulting differential equation assumes the classical form

$$[M] \{\ddot{d}(t)\} + [K] \{d(t)\} = \{F_A(t)\}, \quad (28)$$

where $[M]$ = mass matrix

$[K]$ = stiffness matrix

{d(t)} = displacement vector for the structure

{F_A(t)} = the applied aerodynamic forces.

The basic approach was to ascertain those frequencies at which harmonic motion can exist as a solution to (28).

It is normally convenient in structural analysis applications to work with the frequencies and mode shapes associated with the unexcited structural system.

If we set {F_A(t)} to zero in (28) and assume

$$\{d(t)\} = \{d\} e^{i\omega t}, \tag{29}$$

then (28) becomes, upon rearranging:

$$(\omega^2 I - [M]^{-1} [K]) \{d\} = 0 \tag{30}$$

It is clear therefore that the natural frequencies for the free system correspond to the eigenvalue of [M]⁻¹ [K] and mode shapes {d} correspond to the eigenvectors of [M]⁻¹ [K]. Let us denote the eigenvalues by ω_i and the associated eigenvectors by {p_i}, where i = 1, 2, ... , n. (n is the dimension of {d}.) Define

$$[P] = [\{p_1\} \{p_2\} \dots \{p_n\}] \tag{31}$$

$$[\Omega] = \text{diagonal } [\omega_1^2 \ \omega_2^2 \ \dots \ \omega_n^2]. \tag{32}$$

The natural frequencies in radians per second are tabulated below:

5.241 x 10 ¹⁰	1.305 x 10 ⁹
3.121 x 10 ¹⁰	7.982 x 10 ⁸
1.970 x 10 ¹⁰	5.578 x 10 ⁸
1.320 x 10 ¹⁰	4.788 x 10 ⁸
1.177 x 10 ¹⁰	2.383 x 10 ⁸
7.810 x 10 ⁹	1.121 x 10 ⁷
7.123 x 10 ⁹	5.220 x 10 ⁷
4.483 x 10 ⁹	3.524 x 10 ⁷
4.065 x 10 ⁹	1.992 x 10 ⁶
3.258 x 10 ⁹	5.589 x 10 ⁶
2.151 x 10 ⁹	1.059 x 10 ⁴
1.789 x 10 ⁹	9.588 x 10 ⁴

Table - List of squared natural frequencies - (rad/sec)²

If we return to (28) and assume that the solution $\{d(t)\}$ is written as a linear combination of the basic vectors of $[r]$ with time varying coefficient, we have

$$\{d(t)\} = \sum_{i=1}^n \phi_i(t) \{p_i\} \quad (33)$$

The $\phi_i(t)$ are unknown scalar functions of time. We can place (33) into vector-matrix form by defining

$$\{\phi^T(t)\} = \{\phi_1(t) \cdot \phi_2(t) \dots \phi_n(t)\} \quad (34)$$

and writing

$$\{d(t)\} = [P] \{\phi(t)\} \quad (35)$$

The substitution of (35) into (28), with some manipulations, yields

$$\overset{\circ}{\{\phi(t)\}} + [\Omega] \{\phi(t)\} = [P]^{-1} [M]^{-1} \{F_A(t)\}. \quad (36)$$

It follows therefore that by the introduction of the coordinates ϕ_i , $i = 1, 2, \dots, n$, the left hand side of (36) is decoupled and hence amenable to straight forward solution. However, the right hand side of (36), which has only been written in functional form to this point, is in fact a rather involved function of $\{d(t)\}$. With the substitution of (24) into (36), the dynamical equation for the elastic wing finally becomes:

$$\{-\omega^2 I + [\Omega]\} \{\phi(\omega)\} = \{[S(\omega)] + i\omega[T(\omega)]\} \{\phi(\omega)\} \quad (37)$$

where $[S(\omega)] = \frac{g_\infty}{U_\infty} [P]^{-1} [M]^{-1} [G] [D(\omega)]^{-1} [H] [P]$ (38)

$$[T(\omega)] = \frac{g_\infty}{U_\infty} [P]^{-1} [M]^{-1} [G] [D(\omega)]^{-1} [E] [P]. \quad (39)$$

The inverse Fourier Transform of (37) is

$$\overset{\circ}{\{\phi(t)\}} - [T(t)] * \overset{\circ}{\{\phi(t)\}} + [\Omega] \{\phi(t)\} - [S(t)] * \{\phi(t)\} = 0 \quad (40)$$

where

$$\begin{aligned} [S(t)] &= \mathcal{F}^{-1} \{[S(\omega)]\} \\ [T(t)] &= \mathcal{F}^{-1} \{[T(\omega)]\} \end{aligned}$$

and * denotes the convolution operation. The investigation for instability or sustained oscillation modes for the elastic wing is now reduced to that of finding the location of the roots for the characteristic equation of system (40). Unfortunately, closed form expressions are not available for the elements of $[T(t)]$ and $[S(t)]$ due to the fact that $[D(\omega)]$ can only be computed numerically for specified values of ω . Tests were made to determine if any of the lower natural frequencies corresponded to eigenvalues for (40) and it was determined that they did not.

(IV) Description of Tests

Essentially two types of tests were conducted on the elastic wing after it had been fabricated at the Texas A&M Model Shop.

(A) Static Tests

The vortex lattice program was utilized to compute the aerodynamic loads that could be expected to act on each streamwise row of panels if the wing was rigid. The loads were computed for an angle of attack of 5° and $q_\infty = 80 \text{ lbs/ft}^2$. Weights equal to these spanwise loads were attached to the $1/4$ chord point for each panel section. Then vertical displacement measurements were made for each rib at 25% and 75% of rib length. By using these measurements and data on the unloaded wing position it was possible to calculate the wing elastic pitching rotation.

(B) Wind Tunnel Tests

A series of six wind tunnel tests were conducted at the Texas A&M University Wind Tunnel for two orbiter configurations. The conditions were:

$$\begin{aligned} q_\infty &= 50 \text{ lb/ft}^2; \alpha = 2^\circ, 5^\circ, \& 8^\circ \\ q_\infty &= 80 \text{ lb/ft}^2; \alpha = 2^\circ, 5^\circ, \& 8^\circ \end{aligned}$$

The elevon setting was held at zero for all tests. These tests were conducted for the Orbiter with elastic wings and they were repeated for the Orbiter with

identical rigid wings. The standard force and moment data, C_L , C_D , and C_M , were recorded for each sequence of tests. In addition, a Cathatometer was utilized to make vertical displacement measurements at each spanwise rib location for both the leading and trailing edges of the wing. The Cathatometer was instrumented with a potentiometer so that displacement readings could be automatically read into the wind tunnel digital computer. One difficulty that was experienced during the conduct of the test sequence was that the Cathatometer had to be moved in order to make both leading edge and trailing edge measurements. Due to the unevenness of the floor, the reference point was therefore shifted causing some difficulty in checking test repeatability.

(V) Comparison of Analytical and Experimental Results

As indicated in Section IV, a series of static load tests were conducted to verify that the structural model used for the wing in the computer program was in good agreement with the elastic deformations actually given by the wing. Figures 8 and 9 show curves of vertical deflection and elastic twist about the y axis derived from both experimental and analytical procedures. It is clear that good correlation was obtained for both twist and displacement in the static case, implying that the mathematical characterization of the wing was adequate.

Figures 10, 11, and 12 summarize some of the deformation and force data collected during the wind tunnel program. Figure 10 reflects the expected result that increased rigid angle of attack yielded increased z - direction deformations. Further, for a given q_∞ and α , z - deflections increased uniformly in going from the wing root to the wing tip. Figure 11 provides a comparison of C_L for the elastic and rigid models obtained from experimental procedure. These curves are so close to rigid C_L obtained from the analytical procedure that the latter has been omitted from the Figure. Finally, Figure 12 displays the elastic twist (increment in angle of attack) at $\alpha = 8$ degrees for $q_\infty = 50 \text{ lb/ft}^2$ and 80 lb/ft^2 . It is interesting to observe that a small negative

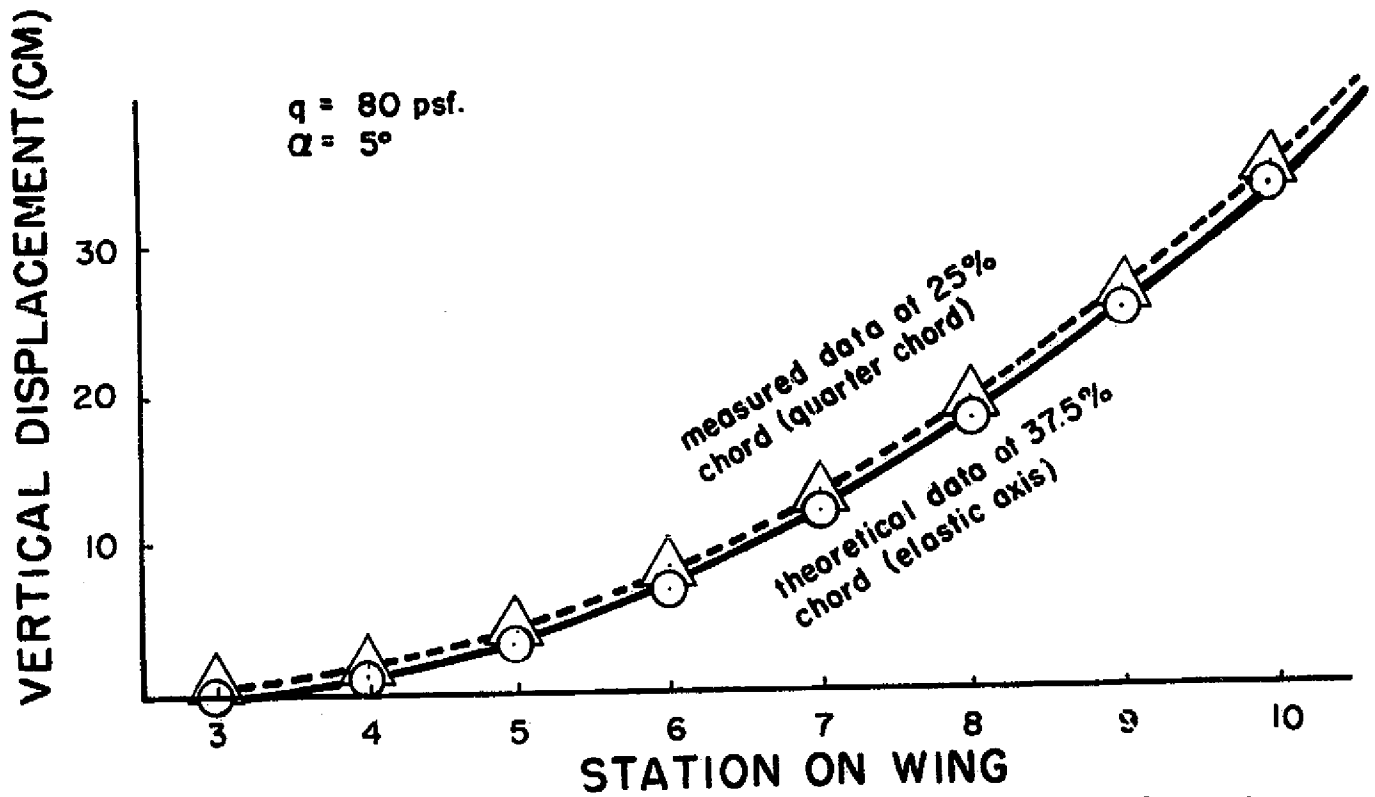


FIGURE 8. Comparison of the static load test linear deflections. Note that the deflection along the leading edge is in general larger than along the trailing edge.

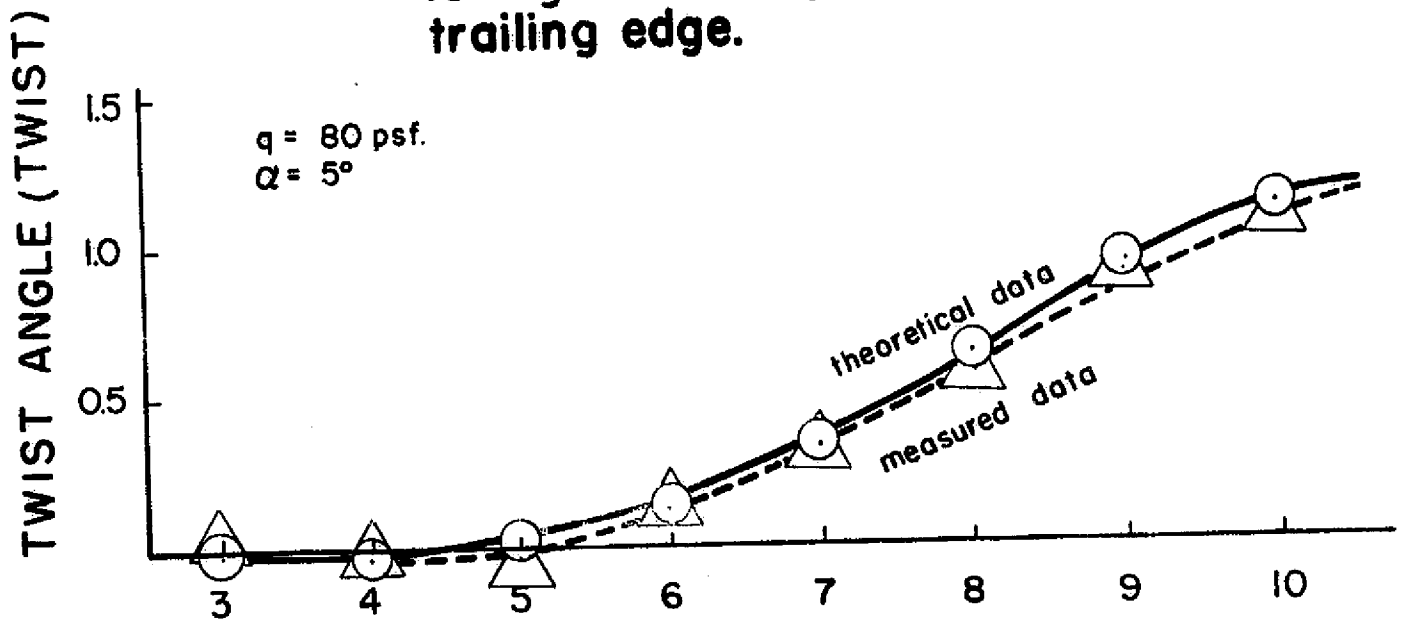


FIGURE 9. Comparison of the static load twist angle.

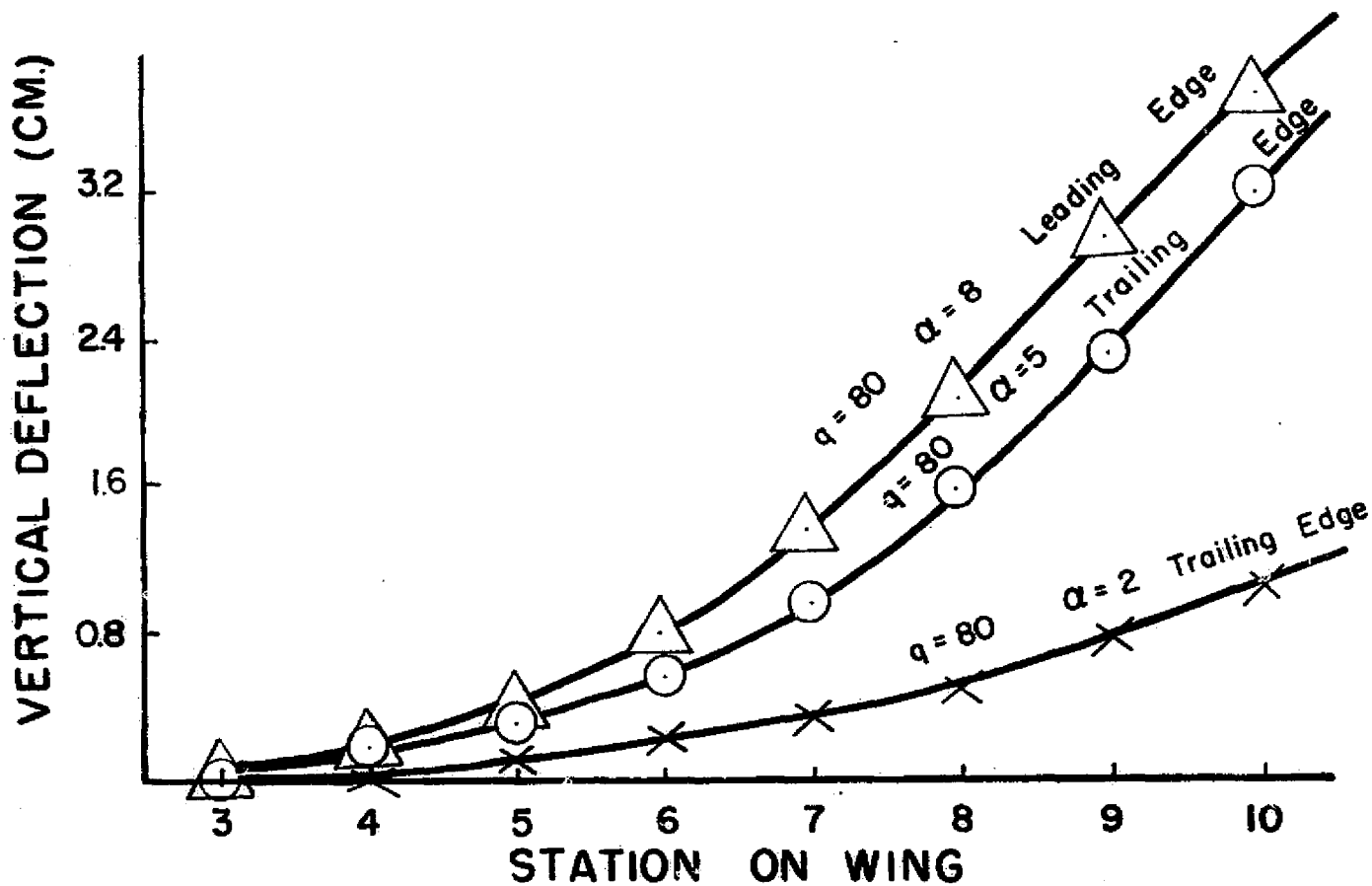


FIGURE 10. Plots of vertical deflections (in centimeters) measured in the wind tunnel.

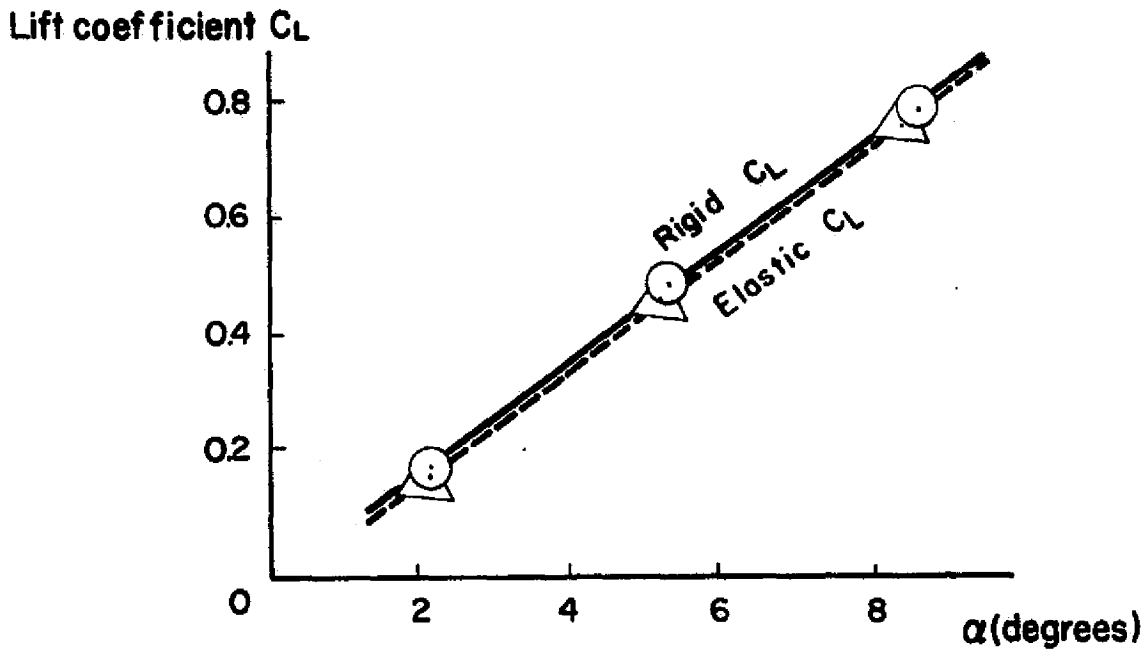


FIGURE II-a. Lift coefficient C_L versus angle of attack α , $q=50$ (leading edge).

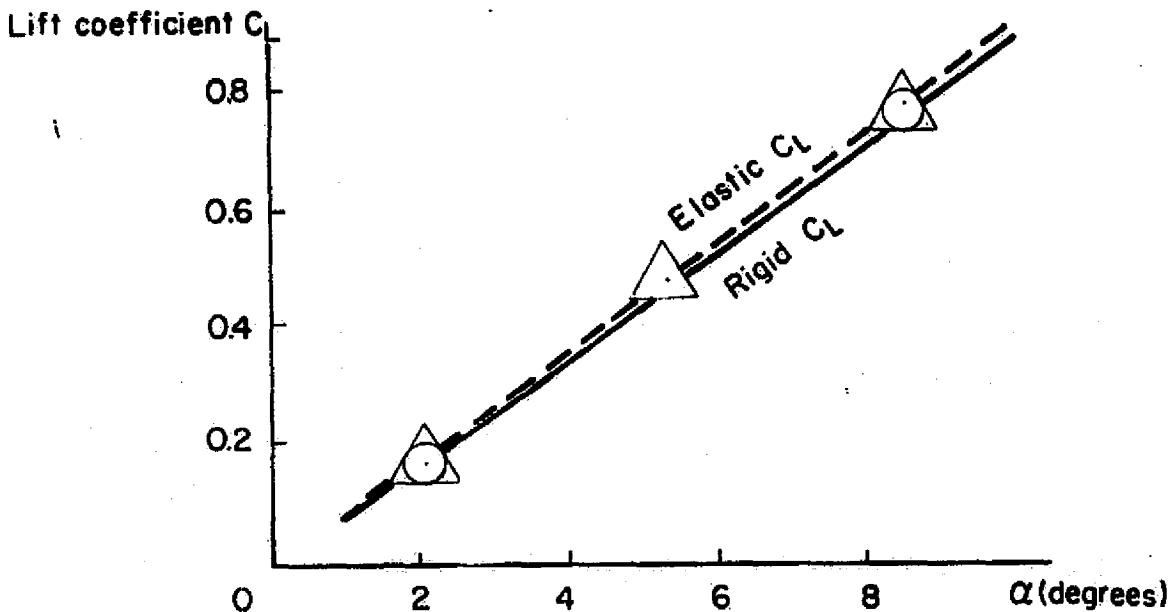


FIGURE II-b. Lift coefficient C_L versus angle of attack α , $q=80$ (leading edge).

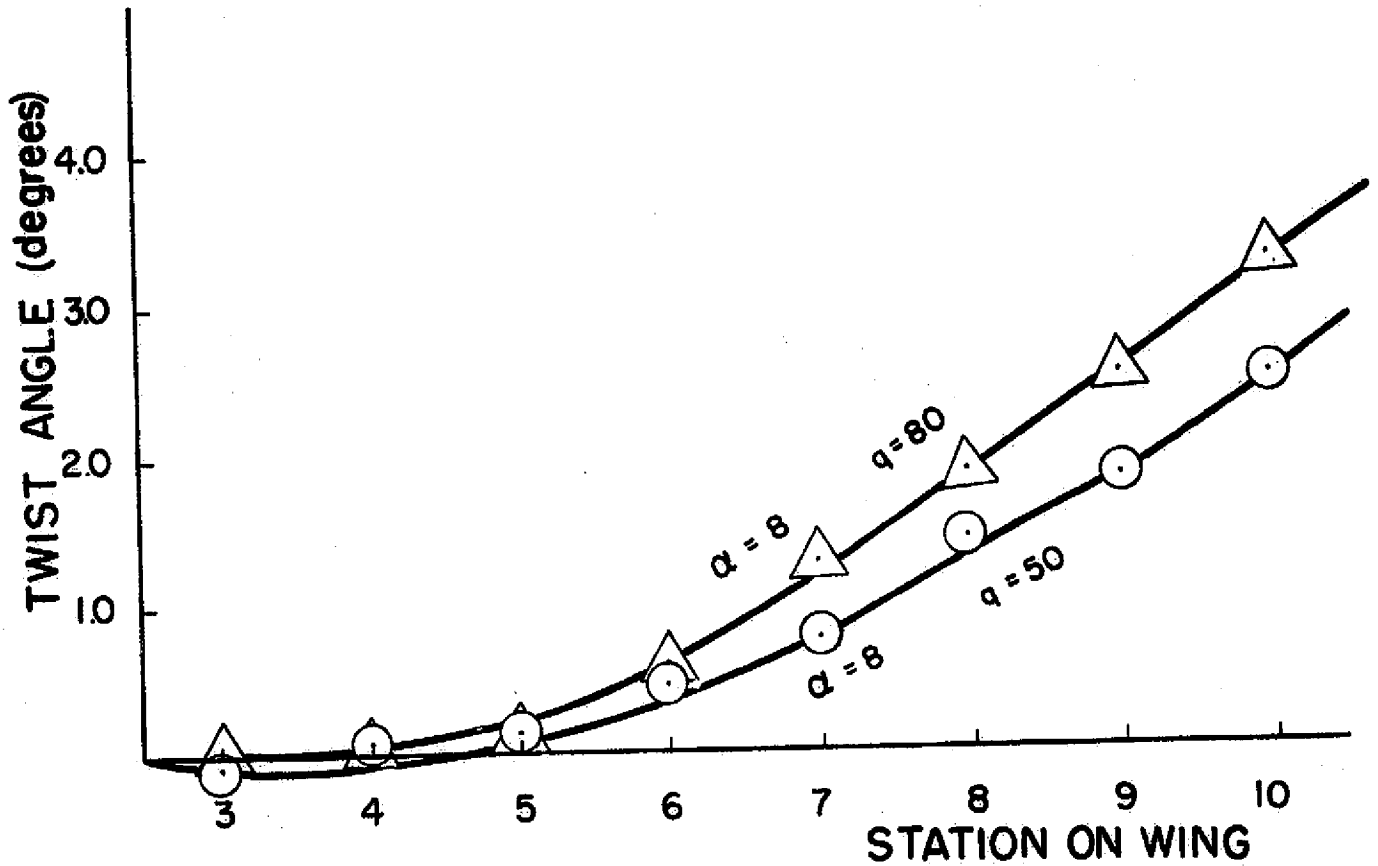


FIGURE 12. Plots of the twist angles measured from the wind tunnel.

angle of twist was measured at some of the inboard wing stations. Appendix B contains a tabulation of Wind Tunnel Test Results.

Finally, we wish to offer a comparison of experimental and theoretical aeroelastic estimates. The theoretical method outlined in Section III-C was used to estimate static aeroelasticity effects. The reader is reminded that the fuselage section of the orbiter was represented aerodynamically as a flat plate whose streamwise length corresponded to that of the wing root. Figure 13 shows a comparison of estimated and measurements for the wing leading edge z deflection. This Figure shows that this particular set of data correlated quite well. However, from Figure 14 we find that the theory estimates for elastic increment in angle of attack lie below those obtained experimentally. In an effort to determine if this difference was due to an inaccurate estimate of local center of pressure for each panel section, the centers of pressure were shifted forward by 20% and a new solution determined. While this does give better agreement, it does not appear that the solution to this discrepancy can be obtained by a simple center of pressure shift.

(VI) Discussion

In this report we have described the design, fabrication, testing, and analysis of a quasi-elastic orbiter model. The elasticity properties were introduced by constructing beam-like straight wings for the wind tunnel model. A standard influence coefficient mathematical model was used to estimate aeroelastic effects analytically. In general good agreement was obtained between the empirical and analytical estimates of the deformed shape. However in the static aeroelasticity case, we found that the physical wing exhibited less bending and more twist than was predicted by theory. Although the cause of this difference is yet unexplained, there are several factors that may have contributed to it:

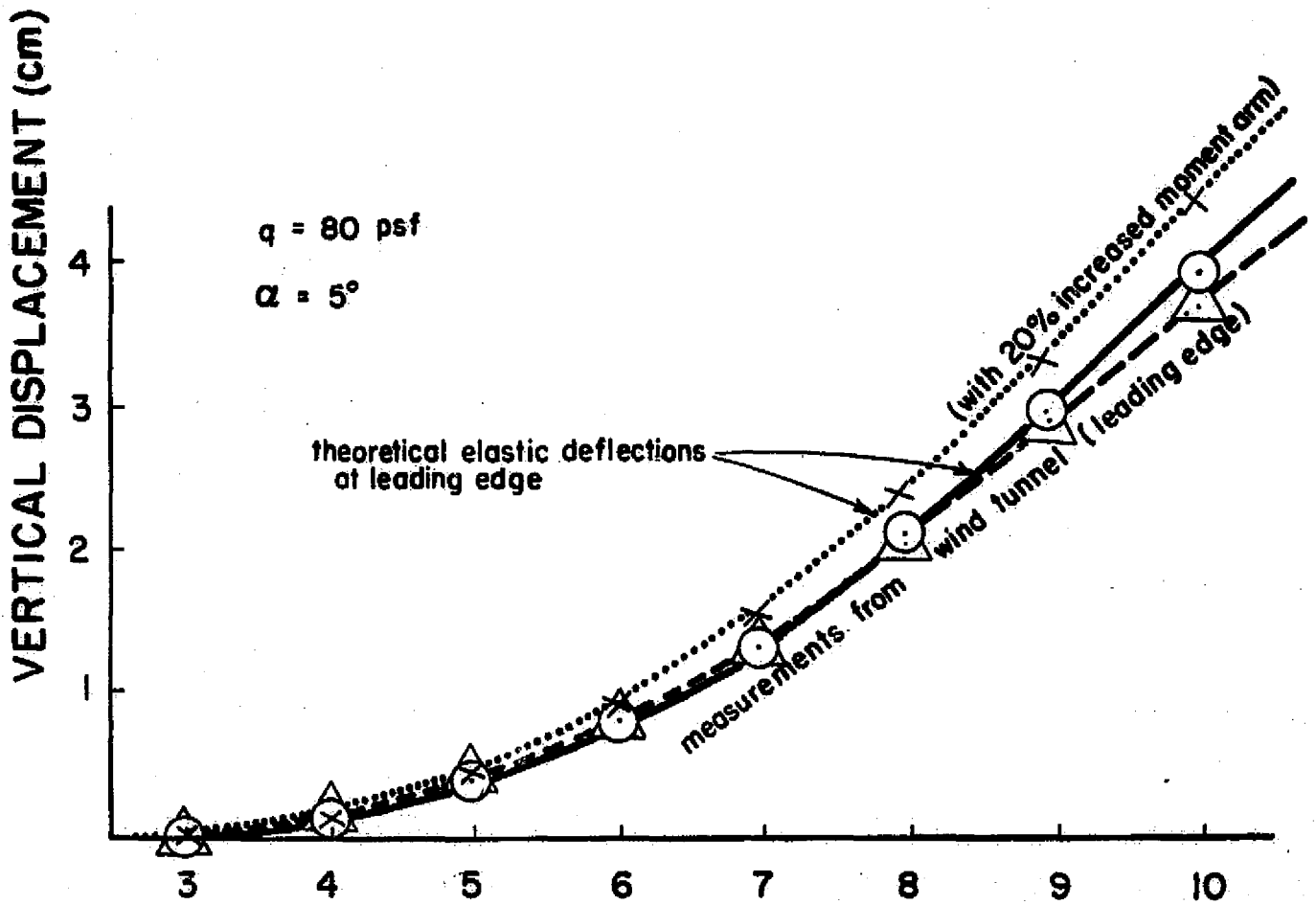


FIGURE 13. Comparison of the elastic deflections.

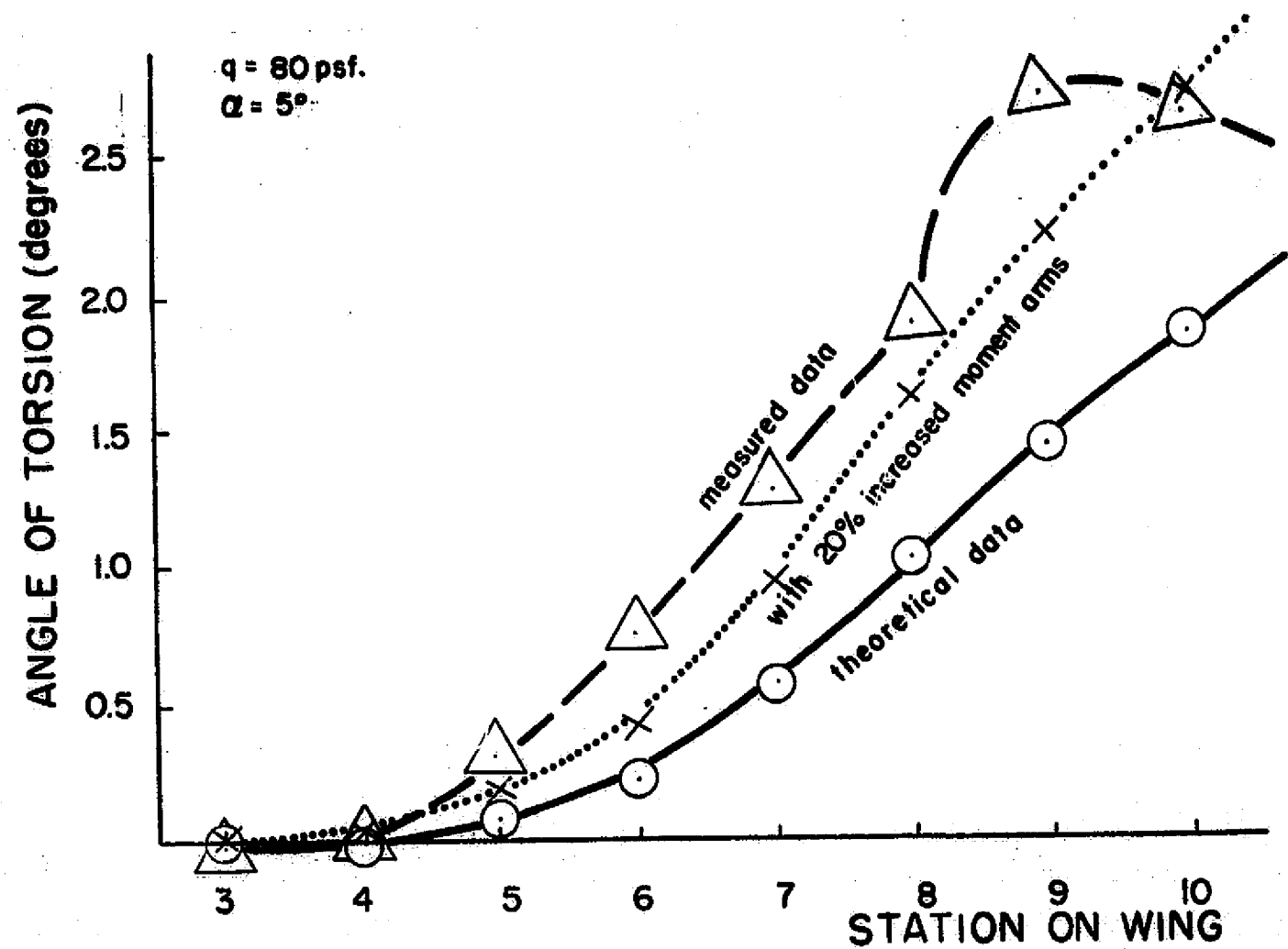


FIGURE 14. Comparison of twist angles.

- 1) Inadequate aerodynamic representation. (See above discussion)
- 2) Imprecise wind tunnel measurements. Although the wing was relatively quiet during testing some induced vibration occurred. This vibration along with cathatometer operator error almost certainly induced an unknown measurement error.
- 3) Structural Integrity. A continual problem that was experienced during testing was that the rib-spar weld joints could easily be destroyed by improper handling. This failure would explain spurious data points like the one at station 9 on Figure 14.
- 4) In-plane bending. The elastic wing was designed to have approximately the same stiffness in-plane as normal to the plane. Since the linear aerodynamic theory provides an inadequate representation for drag, it was not possible to adequately model this effect.

In summary, the results obtained in this report indicate that the linear aerodynamic and theories provide an approximate estimate of aeroelastic effects. However, our results imply that the theory underestimates (at least in this case) the elastic deformation in wing twist and hence the effects of elasticity on lift. We believe that further testing and more complete aerodynamic models are required to resolve this question.

References

- [1] "A Method for Predicting the Stability Characteristic of an Elastic Airplane," Volume I, Theoretical Description by A. R. Dusto and others, D6-41064-1, December 1973.
- [2] J. S. Przemieniecki, "Theory of Matrix Structural Analysis," McGraw-Hill Book Company, (1968).
- [3] J. P. Giesing, T. P. Kalman, and W. P. Rodden, "Subsonic Unsteady Aerodynamics for General Configurations," Technical Report AFFDL-TR-71-5, Part I, Vol. I, (1971).
- [4] I. S. Sokolnikoff, "Mathematical Theory of Elasticity," 2nd ed., New York, McGraw-Hill, 1956.

APPENDIX A

Aeroelasticity Computer Program Listing

The following pages contain a listing of the computer program used to compute the elastic displacements of the model wing.


```

39      IJ=0
40      I2=0
41      DO 890 J=1,N
42      I2=I2+2
43      DO 890 I=1,M
44      IJ=IJ+1
45      I2=I2+1
46      KL=0
47      DO 888 L=1,N
48      DO 888 K=1,MP2
49      KL=KL+1
50      SEDINV(IJ,KL)=DINV(I2,KL)
51      888 CONTINUE
52      890 CONTINUE
53      PRINT 84
54      DO 897 I=1,MN
55      PRINT 46, I
56      PRINT 42, (SEDINV(I,J),J=1,MNT)
57      897 CONTINUE
58      C
59      C      CALL AMAT (M,N,M3,ALPHA,SO, BETA,MSTAR)
60      C
61      C      PRINTOUT THE A-MATRIX
62      PRINT 86
63      DO 900 I=1,M3
64      PRINT 46, I
65      PRINT 40, (A(I,J),J=1,MSTAR)
66      900 CONTINUE
67      C
68      C      READ IN INPUT-DATA
69      READ 52, (GJ(J),J=1,M)
70      READ 52, (EI(J),J=1,M)
71      READ 50, (PLSPAR(J),J=1,M)
72      DO 7 I=1,M
73      GJ(I)=GJ(I)*1.120
74      7 CONTINUE
75      C
76      C      PRINT OUT INPUT-DATA
77      PRINT 70
78      PRINT 74
79      PRINT 54, (GJ(J),J=1,M)
80      PRINT 76
81      PRINT 54, (EI(J),J=1,M)
82      PRINT 78
83      PRINT 40, (PLSPAR(J),J=1,M)
84      C
85      DO 14 I=1,M3
86      DO 14 J=1,M3
87      14 STIFF(I,J)=0.
88      MM1=M-1
89      C
90      C      FORM GLOBAL STIFFNESS AND MASS MATRICES
91      DO 32 I1=1,MM1
92      I3M3=I1*3-3
93      IF(I1.GT.1)GO TO 919
94      C
95      CALL STIFFE (ESTIFF,GJ(I1),EI(I1),1,NF)
96      CALL TRFORM (ESTIFF,THETA 1,NF)
97      CALL STIFFE (ESTIFF,GJ(2),EI(2),2,NF)
98      CALL TRFORM (ESTIFF,THETA 1,NF)

```

```

C
89   NFD2=NF/2
90   DO 646 I=1,NFD2
91   DO 646 J=1,NFD2
92   ESTIFF(I,J)=ESTIFF(I,J)+E*IF1(I+NFD2,J+NFD2)
93   646 CONTINUE
94   GO TO 929
95   919 CONTINUE
96   IIP1=I+1
C
97   CALL STIFFE (ESTIFF,GJ(IIP1),F1(IIP1),IIP1,NF)
98   CALL TRFORM (ESTIFF,THETA 1,NF)
C
99   929 CONTINUE
C
100  COMBINE ELEMENTAL MATRICES INTO GLOBAL MATRIX
101  DO 13 J1=1,NF
102  DO 13 K1=1,NF
103  STIFF(I3M3+J1,I3M3+K1)=STIFF(I3M3+J1,I3M3+K1)+ESTIFF(J1,K1)
104  13 CONTINUE
105  32 CONTINUE
C
106  PRINT OUT THE STIFF-MATRIX
107  PRINT B2
108  DO 280 I=1,M3
109  PRINT 46, I
110  PRINT 54, (STIFF(I,J),J=1,M3)
111  280 CONTINUE
C
112  MATRIX K- MATRIX A
C
113  DO 310 I=1,M3
114  DO 310 J=1,M3
115  DIFF(I,J)=STIFF(I,J)-A(I,J)
116  310 CONTINUE
117  GOTO 320
118  PRINT 88
**WARNING** UNNUMBERED EXECUTABLE STATEMENT FOLLOWS A TRANSFER
119  DO 311 I=1,M3
120  PRINT 46, I
121  PRINT 54, (DIFF(I,J),J=1,M3)
122  311 CONTINUE
123  320 CONTINUE
C
124  CALL INVET (DIFF,M3,1.006)
C
125  GENERALIZED DISPLACEMENTS
126  DO 332 I=1,M3
127  VEC2(I)=0.0
128  DO 332 J=1,MSTAR
129  VEC2(I)=VEC2(I)+A(I,J)*ALPHA
130  332 CONTINUE
131  DO 360 I=1,M3
132  EDP(I)=0.0
133  DO 360 J=1,M3
134  EDP(I)=EDP(I)+DIFF(I,J)*VEC2(J)
135  360 CONTINUE
C
136  PRINT OUT DISPLACEMENT VECTOR
137  PRINT 72

```

ORIGINAL PAGE IS
OF POOR QUALITY


```

132 PRINT R0
133 PRINT Q1
134 PRINT 44, (EDP(L),L=1,M3)
135 PRINT 72
136 PRINT 94
137 PRINT 95
138 DO 400 I=1,M
139 J=(I-1)*3+1
140 K=(I-1)*3+2
141 L=(I-1)*3+3
142 PRINT 44, FDP(J)*2.540 +RIBUH(I )*EDP(L)*2.540 ,EDP(K)*57.2
      I 95780,EDP(L)*57.295780

```

EXTENSION OTHER COMPILERS MAY NOT ALLOW EXPRESSIONS IN OUTPUT LISTS
EXTENSION OTHER COMPILERS MAY NOT ALLOW EXPRESSIONS IN OUTPUT LISTS
EXTENSION OTHER COMPILERS MAY NOT ALLOW EXPRESSIONS IN OUTPUT LISTS

```

143 400 CONTINUE
144 PRINT 72
145 PRINT 94
146 PRINT 95
147 DO 420 I=1,M
148 J=(I-1)*3+1
149 K=(I-1)*3+2
150 L=(I-1)*3+3
151 PRINT 44, FDP(J)*2.540 -RIBUH(I )*EDP(L)*2.540 ,FDP(K)*57.2
      I 95780,EDP(L)*57.295780

```

EXTENSION OTHER COMPILERS MAY NOT ALLOW EXPRESSIONS IN OUTPUT LISTS
EXTENSION OTHER COMPILERS MAY NOT ALLOW EXPRESSIONS IN OUTPUT LISTS
EXTENSION OTHER COMPILERS MAY NOT ALLOW EXPRESSIONS IN OUTPUT LISTS

```

152 420 CONTINUE
      C
153 99 STOP
154 END
      C
      *****

```

```

155 SUBROUTINE DLY (PETA,SO,ALPHA,N)
      C
      C THE DOUPLET LATTICE PROCEDURE
      C FOR STEADY-PLANAR, SUBSONIC, COMPRESSIBLE FLOW.
      C
      C INCREMENTAL OSCILLATORY DOWNWASH FACTORS
      C (BY FITTING THE KERNEL FUNCTION FOR LIFTING FUNCTIONS WITH A PARABOLA)
      C
      C SYMBOLS:
      C ALPHA =STATIC ANGLE OF ATTACK
      C R0TLE=LOCATION OF THE ROOT POINT ON LEADING EDGE
      C R0TTE=LOCATION OF THE ROOT POINT ON TRAILING EDGE
      C T0LE=LOCATION OF THE TIP POINT ON LEADING EDGE
      C T0TE=LOCATION OF THE TIP POINT ON TRAILING EDGE
      C M =NUMBER OF COLUMNS OF WING PANELS (ON ONE WING)
      C N =NUMBER OF PANELS PER COLUMN
      C (THE COLUMNS RUN FROM THE LEADING TO TRAILING EDGE OF THE WING)
      C B =LENGTH OF SEMI-WING SPAN
      C PERC(I)=PERCENTAGE OF CHORDWISE LOCATION ON THE WING
      C PERC(J)=PERCENTAGE OF SPAN-WISE LOCATION ON THE WING
      C X0(I,J)=LENGTH OF EACH DOUPLET LINE
      C DELA(I,J)=AREA OF EACH WING PANEL
      C X1(I,J)=LOCATION OF EACH SENDING POINT ONT EACH PANEL
      C X (I,J)=LOCATION OF RECEIVING POINT ON EACH PANEL
      C AXSLP =SLOPE OF MAJOR AXIS OF THE WING
      C XIAX(J)=XI COORDINATES OF EACH COLUMN ALONG THE MAJOR AXIS

```

ORIGINAL PAGE IS
OF POOR QUALITY

```

C          DELCP(I)=PRESSURE COEFFICIENTS ON ONE WING
C          VA      =SPEED OF SOUND
C          FMACH   =FREE STREAM MACH NUMBER
C          UINF    =FREE STREAM VELOCITY
C
156      IMPLICIT REAL*8 (A-H,O-Z)
157      DIMENSION PCVSLP(6),SLOPE(6),PERCS(11),PEPCC(7)
158      DIMENSION XIIP(6),XIOP(6),XIID(6),XIID(6),TANLAM(7)
159      DIMENSION XII(7),XIO(7),Y(10),ETAC(10),XIAX(10),C(11),ETA(11)
160      DIMENSION XI(6,10),XIC(6,10),X(6,10)
161      DIMENSION DELPI(6,10),DELX(6,10), R(6,10)
162      DIMENSION DELC(6,11)
163      REAL*8 LAMDA(6),LAMBDA(6),MU(6,10),ILEFT,IRIGHT
164      COMMON /AREA3/ DRSS(60,60),RTRUM(10),RIRLH(10)
165      COMMON /AREA5/ DELA(6,10),FL(6,10)
C
166      200 READ (5,210,END=990) ROOTLE,ROOTTE,TIPLE,TIPTE,B,N,M,ALPHA
167      210 FORMAT (5F10.3,2I10,F10.6)
168      PRINT 220
169      220 FORMAT ('1')
170      PRINT 230
171      230 FORMAT (4X,'DATA INPUT:- ')
172      PRINT 240, ROOTLE,ROOTTE,TIPLE,TIPTE,B,M,N
173      240 FORMAT (4X,'ROOTLE= ',F10.4,4X,'ROOTTE= ',F10.4,4X,'TIPLE= ',F10.4
174      1      ,4X,'TIPTE= ',F10.4,4X,'B= ',F10.4,4X,'M= ',I4,4X,'N= ',I4)
175      PRINT 250, ALPHA
176      250 FORMAT ('-',4X,'ANGLE OF ATTACK IS ',F10.6)
C
176      VA=1090.0
177      W=0.0
178      WK=0.0
179      UINF=250.0
180      FMACH=UINF/VA
181      BETA=DSQRT(1.0-FMACH**2)
182      R=R*BETA
183      SQ=0.50#0.002503867*UINF**2
C
184      PRINT 252, FMACH,BETA,SQ
185      252 FORMAT (T20,'MACH NUMBER=',F10.6,T60,'BETA=',F10.6,T90,'DYNAMIC PR
PRESSURE, Q=',F10.3)
C
C          PRECALCULATION FOR THE COORDINATES OF THE SENDING AND RECEIVING ELEMENTS
C          CALCULATION OF THE AREA OF EACH WING PANEL
C
186      IN=N+1
187      IM=M+1
188      MN=M*N
189      READ 254, (PERCS(J),J=1,IM)
190      READ 254, (PEPCC(I),I=1,IN)
191      254 FORMAT (8F10.6)
192      PRINT 250
193      250 FORMAT ('-',4X,'PERCENT OF SPANWISE PANELING LOCATION')
194      PRINT 305, (PERCS(J),J=1,IM)
195      PRINT 260
196      260 FORMAT ('-',4X,'PERCENT OF CHORDWISE PANELING LOCATION')
197      PRINT 305, (PEPCC(I),I=1,IN)
198      DO 270 J=1,IM
199      ETA(J)=R*PERCS(J)
200      270 CONTINUE
201      DO 280 I=1,IN
202      XII(I)=(ROOTTE-ROOTLE)*PERCC(I)+ROOTLE

```

```

203      XI(I)=(TIPF-TIPLE)*PERCC(I)+TIPLE
204      TANLAM(I)=(XI(I)-XIII(I))/B
205  280 CONTINUE
206      C(I)=ROOTLE-ROOTLE
207      C(IM)=TIPF-TIPLE
208      AXSLP=(TIPLE-ROOTLE+0.3750)*(C(IM)-C(I))/B
209      AXDEG=57.295780*DATAN(AXSLP)
210      PRINT 284, AXDEG
211  284 FORMAT ('-', 'SLOPE OF MAJOR AXIS =', F16.6, ' DEGREES')
C
C      SLOPE OF LINE DOUBLETS, SLOPE, WITH ITS ANGLE, LAMDA.
212  DO 370 I=1, N
213  DO 300 J=1, IM
214      C(I)=C(I)-(C(I)-C(IM))*PERCC(J)
215      DELC(I, J)=(PERCC(I+1)-PERCC(I))*C(J)
216  300 CONTINUE
217      XIID(I)=XIII(I)+0.250 *DELC(I, I)
218      XIID(IM)=XIII(IM)+0.250*DELC(I, IM)
219      SLOPE(I)=(XIID(IM)-XIID(I))/B
220      LAMDA(I)=DATAN(SLOPE(I))
221      LAMDA(I)=LAMDA(I)+57.295780
222      XIIR(I)=XI(I)+0.750 *DELC(I, I)
223      XIIR(IM)=XI(IM)+0.750 *DELC(I, IM)
224  370 RCVSLP(I)=(XIIR(IM)-XIIR(I))/B
225      PRINT 300
226  380 FORMAT ('-', 4X, 'ANGLE OF EACH DOUBLET LINE (IN DEGREES)')
227      PRINT 305, (LAMDA(I), I=1, N)
228  305 FORMAT (4X, F16.6)
C
C
C      NOW COMPUTING THE REQUIRED COORDINATES
229  IJ=0
230  DO 405 I=1, N
231  DO 405 J=1, M
232      MU(I, J)=(ETA(J+1)-ETA(J))/DCOS(LAMDA(I))
233      INDEXJ=2*(M-J)+1
234      DELA(I, J)=0.5000*DELC(I, J)*(ETA(J+1)-ETA(J))*(C(I)*INDEXJ
1      +C(IM)*(2*M-J))/C(I)*M
235      DELA(I, J)=DELA(I, J)/BETA
236      IJ=IJ+1
237      XI(I, J)=XIID(I)+ETA(J) *SLOPE(I)
238      ETAC(J)=0.50*(ETA(J)+ETA(J+1))
239      Y(J)=ETAC(J)
240      XI(I, J)=XIIR(I)+RCVSLP(I)*Y(J)
241      DELX(I, J)=0.50*(DELC(I, J)+DELC(I, J+1))
242      XI(I, J)=XI(I, J)-0.50*DELX(I, J)
243      XIAX(J)=0.3750*C(I)+AXSLP*Y(J)+ROOTLE
244      FL(I, J)=XI(I, J)-XIAX(J)
245      R(I, J)=XI(I, J)-XIAX(J)
246      RIBUH(J)=(C(I)+C(J+1))/2.0*0.3750
247      FIPUH(J)=RIBUH(J)+0.6250/0.3750
248  405 CONTINUE
249      PRINT 308
250  308 FORMAT ('-', 'XI-LOCATIONS ALONG THE MAJOR AXIS:--')
251      PRINT 340, (XIAX(K), K=1, M)
252      PRINT 310
253  310 FORMAT ('-', 4X, 'HERE IS THE VECTOR OF M')
254  DO 311 I=1, N
255      PRINT 330
256      PRINT 340, (MU(I, J), J=1, M)

```

ORIGINAL PAGE IS
OF FOUR EQUALS

```

257 311 CONTINUE
C PRINT 314
C 314 FORMAT ('-',4X,'X-LOCATIONS OF EACH RECEIVING POINT')
C PRINT 330
C PRINT 340, ((X(I,J),J=1,M),I=1,N)
259 PRINT 320
259 320 FORMAT ('-',4X,'PANEL AREA ON ONE WING')
260 DO 350 I=1,N
261 PRINT 330
262 330 FORMAT ('-')
263 PRINT 340, (OFLA(I,J),J=1,M)
264 340 FORMAT (4X,10F12.6)
265 350 CONTINUE
266 PRINT 352
267 352 FORMAT ('-',T20,'L(I,J) WITH SIGN OF THEIR X-COORDINATE LOCATION B
BEING CARRIED ALONG')
268 DO 353 I=1,N
269 PRINT 330
270 PRINT 340, (FL(I,J),J=1,M)
271 353 CONTINUE
272 PRINT 354
273 354 FORMAT ('-',T20,'R(I,J) WITH SIGN OF THEIR X-COORDINATE LOCATION B
BEING CARRIED ALONG')
274 DO 355 I=1,N
275 PRINT 330
276 PRINT 340, (P(I,J),J=1,M)
277 355 CONTINUE
C
C NOW CALCULATE DRS(1) AND DRS(S) MATRICES
C PRINT 360
C 360 FORMAT ('-',18X,'DRSS',20X,'DRS1')
278 T1=1.0
279 KL=0
280 DO 590 K=1,N
281 DO 590 L=1,M
282 KL=KL+1
283 IJ=0
C PRINT 415
C 415 FORMAT ('-')
C PRINT 363, KL
284 DO 580 I=1,N
C PRINT 315
C 315 FORMAT (4X,' ')
DO 580 J=1,M
285 IJ=IJ+1
286 XMXI=X(K,L)-XI(I,J)
287 YMETA= Y(L)-ETA(IJ)
288 YPETA=Y(L)+ETA(IJ)
289 XMXC=X(K,L)-XIC(I,J)
290 YMETAC= Y(L)-ETAC(IJ)
291 YPETAC=Y(L)+ETAC(IJ)
292 ROOT= DSORT(MU(I,J)**2-2.0 *(XMXI*DSIN(LAMDA(I))
293 +YMETA*DCOS(LAMDA(I)))*MU(I,J)+XMXI**2+YMETA**2)
294 IRIGHT=MU(I,J)/(YMETA+(Y(L)-ETA(J+1)))+(ROOT/(Y(L)-ETA(J+1)))
1 - DSORT(XMXI**2+YMETA**2)/YMETA)/(XMXI*DCOS(LAMDA(I))
2 -YMETA*DSIN(LAMDA(I)))
295 ROOT= DSORT(MU(I,J)**2-2.0 *(XMXI*DSIN(LAMDA(I))
296 +YPETA*DCOS(LAMDA(I)))*MU(I,J)+XMXI**2+YPETA**2)
1 ILEFT=MU(I,J)/(YPETA+(Y(L)+ETA(J+1)))-(ROOT/(Y(L)+ETA(J+1)))
1 - DSORT(XMXI**2+YPETA**2)/YPETA)/(XMXI*DCOS(LAMDA(I))

```

```

2      +YPETA*DSIN(LAMDA(I))
C      DRSS=(IRIGHT+ILEFT)*DCOS(LAMDA(I))
C      IF (W.EQ.0.0) GOTO 492
297    DRSS(KL,IJ)=(IRIGHT+ILEFT)*DCOS(LAMDA(I))
298    DRSS(KL,IJ)=DRSS(KL,IJ)*0.50*DELX(I,J)/4.0/3.14159265360
C
C      TRANSFORM BACK TO THE ORIGINAL Y-AXIS
299    YMETA=YMETA/BETA
300    YPETA=YPETA/BETA
301    YMETAC=YMETAC/BETA
302    YPETAC=YPETAC/BETA
303    580 CONTINUE
304    590 CONTINUE
C
305    CALL INVPT (DRSS,MN,1.000)
C
306    DO 600 I=1,N
307    DO 600 J=1,M
308    FL (I,J)=FL (I,J)/BETA
309    600 CONTINUE
310    GOTO 200
311    900 CONTINUE
312    RETURN
313    END
C
*****
314    SUBROUTINE STIFF (ESTIFF,EGJ,EEI,N,NF)
315    IMPLICIT REAL*8 (A-H,O-Z)
316    DIMENSION ESTIFF(NF,NF)
317    COMMON /AR41/ RLSPAR(8)
C
318    RLC =RLSPAR(N)
319    RLC2=RLC**2
320    RLC3=RLC**3
C
C      FORM BENDING STIFFNESS MATRIX-
321    DO 40 I=1,NF
322    DO 40 J=1,NF
323    ESTIFF(I,J)=0.0
324    40 CONTINUE
325    ESTIFF(1,1)=12./RLC3*EEI
326    ESTIFF(1,2)=6./RLC2*EEI
327    ESTIFF(1,4)=-12./RLC3*EEI
328    ESTIFF(1,5)=6./RLC2*EEI
329    ESTIFF(2,1)=ESTIFF(1,2)
330    ESTIFF(2,2)=4./RLC*EEI
331    ESTIFF(2,4)=-6./RLC2*EEI
332    ESTIFF(2,5)=2./RLC*EEI
333    ESTIFF(4,1)=ESTIFF(1,4)
334    ESTIFF(4,2)=ESTIFF(2,4)
335    ESTIFF(4,4)=ESTIFF(1,1)
336    ESTIFF(4,5)=-6./RLC2*EEI
337    ESTIFF(5,1)=ESTIFF(1,5)
338    ESTIFF(5,2)=ESTIFF(2,5)
339    ESTIFF(5,4)=ESTIFF(4,5)
340    ESTIFF(5,5)=ESTIFF(2,2)
C
C      FORM TORSIONAL STIFFNESS MATRIX-
341    ESTIFF(3,3)=EGJ/RLC
342    ESTIFF(6,3)=-EGJ/RLC

```

ORIGINAL PAGE IS
OF POOR QUALITY

```

343 ESTIFF(3,6)=ESTIFF(6,3)
344 ESTIFF(6,6)=ESTIFF(3,3)
345 RETURN
346 END
C *****

```

```

347 SUBROUTINE TRFORM (A,THETA,NF)
348 IMPLICIT REAL*8 (A-H,O-Z)
349 DIMENSION A(NF,NF),TRANS(6,6),PROD(6,6)

```

```

C
350 DO 44 I=1,NF
351 DO 44 J=1,NF
352 44 TRANS(I,J)=0.0
353 TRANS(1,1)=1.0
354 TRANS(4,4)=1.0
355 TRANS(2,2)=DCOS(THETA)
356 TRANS(2,3)=-DSIN(THETA)
357 TRANS(3,2)=DSIN(THETA)
358 TRANS(3,3)=DCOS(THETA)
359 TRANS(5,5)=DCOS(THETA)
360 TRANS(5,6)=-DSIN(THETA)
361 TRANS(6,5)=DSIN(THETA)
362 TRANS(6,6)=DCOS(THETA)
363 DO 51 I=1,NF
364 DO 51 J=1,NF
365 PROD(I,J)=0.
366 DO 52 K=1,NF
367 52 PROD(I,J)=PROD(I,J)+TRANS(K,I)*A(K,J)
368 51 CONTINUE
369 DO 53 I=1,NF
370 DO 53 J=1,NF
371 A(I,J)=0.0
372 DO 54 K=1,NF
373 54 A (I,J)=A (I,J)+PROD(I,K)*TRANS(K,J)
374 53 CONTINUE
375 RETURN
376 END
C *****

```

```

377 SUBROUTINE AMAT (M,N,M3,ALPHA,SO, BETA,MSTAR)

```

```

C
C SYMBOLS:-
C THETA1 =ANGLE FROM ELASTIC AXIS ONTO THE Y-AXIS
C THETA2 =ANGLE FROM LINE OF LOADINGS ONTO THE Y-AXIS
C B =SEMI-SPANWISE LENGTH
C ROOTLE =LOCATION OF THE ROOT POINT ON LEADING EDGE
C ROOTTE =LOCATION OF THE ROOT POINT ON TRAILING EDGE
C TIPLE =LOCATION OF THE TIP POINT ON LEADING EDGE
C TIPTT =LOCATION OF THE TIP POINT ON TRAILING EDGE
C ATDEG =ANGLE OF ATTACK IN DEGREES
C FXF(L1) =VERTICAL FORCE LOAD ONTO THE J-TH. SECTION OF THE WING
C FXF(L2) =BENDING MOMENT LOAD ONTO THE WING (EQUALS ZERO IN HERE)
C FXF(L3) =TORSIONAL MOMENT LOAD ONTO THE J-TH. SECTION OF THE WING
C (CAUSED BY VERTICAL FORCE APPLIED OFF FROM THE MAJOR AXIS)
C Y(J) =Y-LOCATION OF EACH WING SECTION
C XAX(J) =X-LOCATION ALONG THE MAJOR AXIS
C XLD(J) =X-LOCATION ALONG THE LINE OF LOADING ON THE WING
C ARM(J) =TORSIONAL MOMENT ARM OF THE J-TH. SECTION
C RIC =SPANWISE LENGTH OF EACH PANEL
C FF(I,J) =CONDENSED CIRCULATION MATRIX

```

```

C      RPD(J)      =DISTANCE OF DYNAMIC PRESSURE OFF FROM THE MAJOR AXIS
C
378      IMPLICIT REAL*8 (A-H,O-Z)
C      DIMENSION ETA(MP1)
379      DIMENSION ETA(9),DPC(8),FLD(48)
380      DIMENSION ARM(3),F(8,10), XAX(8),XLD(8),Y(8)
381      DIMENSION CLAI( 8,10),DEL CP(48,10)
382      COMMON /AREA2/ TPETA1
383      COMMON /AREA4/ RPDINV(48,60),A(24,30)
384      COMMON /AREA5/ DELA(6,10),FL( 6,10)
C
385      2 FORMAT (8F10.6)
386      8 FORMAT ('-',4X,'ACTUAL MOMENT ARM OF EACH COLUMN (ALONG THE SPAN)')
C
387      THETA2=0.20362
388      ROOTLC=0.0
389      ROOTTE=10.0050
390      TIPTE=10.0050
391      TIPLE=5.980
392      R=21.84
C
C      CALCULATE DISTANCE OFF FROM THE MAJOR AXIS OF EACH STATION
393      MP1=M+1
394      MP2=M+2
395      MSTAR=M*3+6
396      DO 30 J=1,MP1
397      ETA(J)=R*(J-1)/M
398      30 CONTINUE
399      DO 40 J=1,M
400      Y(J)=0.50*(ETA(J)+ETA(J+1))
401      X AX(J)=ROOTLC+0.3750*(RCOTTE-ROOTLC)+Y(J)*DTAN(THETA1)
402      X LD(J)=ROOTLC+0.250 *(RCOTTE-ROOTLC)+Y(J)*DTAN(THETA2)
403      XA(J)=X AX(J)-X LD(J)
404      40 CONTINUE
405      MN=M*N
406      DO 43 I=1,MN
407      DO 43 J=1,MP2
408      DEL CP(I,J)=0.0
409      DO 42 K=1,N
410      L=(K-1)*MP2
411      DEL CP(I,J)=DEL CP(I,J)-RPDINV(I,J+L)
412      43 CONTINUE
413      43 CONTINUE
414      DO 45 I=1,M
415      DO 45 J=1,MP2
416      CLAI(I,J)=0.0
417      DO 44 K=1,N
418      L=(K-1)*M
419      CLAI(I,J)=CLAI(I,J)+DEL CP(I+L,J)/BETA*DELA(K,I+2)
420      44 CONTINUE
421      F (I,J)=CLAI(I,J)*SQ/144.0
422      45 CONTINUE
C
C      FIND THE EXACT LOCATION OF DYNAMIC PRESSURE
423      MNES=MP2*N
424      DO 60 I=1,MN
425      FLD(I)=0.0
426      DO 60 J=1,MNES
427      FLD(I)=FLD(I)-RPDINV(I,J)

```

ORIGINAL PAGE IS
OF POOR QUALITY

```

428      60 CONTINUE
429      DO 65 I=1,M
430      REP1=0.0
431      REP2=0.0
432      DO 62 I=1,N
433      K=(I-1)*M+J
434      FLD(K)=FLD(K)*DELA(I,J+2)/BETA
435      FLD(K)=FLD(K)*SQ/144.0
436      REP1=REP1+FLD(K)
437      REP2=REP2-FL(I,J+2)*FLD(K)
438      62 CONTINUE
439      DPC(J)=REP2/REP1
440      DPC(J)=DPC(J)*1.20
441      65 CONTINUE

C
C      PRINT OUT THE MOMENT ARM
442      PRINT 8
443      PRINT 2, (DPC(J),J=1,M)

C
C      COMPARE TO THE QUATER CHORD MOMENT ARM
444      PRINT 2, (ARM(J),J=1,M)

C
C      FORM COEFFICIENT MATRIX FOR EXTERNAL LOAD
445      DO 50 I=1,M3
446      DO 50 J=1,*STAP
447      A(I,J)=0.0
448      50 CONTINUE
449      DO 55 I=1,M
450      ARM(I)=DPC(I)
451      I3=I*3
452      DO 55 J=1,M3
453      J3=J*3
454      A(I3-2,J3)=F(I,I)
455      A(I3,J3)=F(I,J)*ARM(I)*DCOS(ALPHA)
456      55 CONTINUE
457      RETURN
458      END

C
*****

459      SUBROUTINE INVPT(A,N,SCALE)
460      IMPLICIT REAL*8 (A-H,O-Z)
461      DIMENSION A(N,N),INDEX(90,2),IPVOT(90),PIVOT(90)
C      CALL FRRSPT(207,256,0,1)

C
C      SCALE DOWN MATRIX A
462      DO 1 I=1,N
463      DO 1 J=1,N
464      1 A(I,J)=A(I,J)/SCALE
465      ONE=1.0
466      ZERO=0.0
467      67 DET=ONE
468      DO 17 J=1,N
469      17 IPVOT(J)=0
470      DO 135 I=1,N
C      FOLLOWING 12 STATEMENTS FOR SEARCH FOR TIVOT ELEMENT
471      T=ZERO
472      DO 9 I=1,N
473      F=(IPVOT(I)-1) 13,9,13
474      13 DO 23 K=1,N
475      F=(IPVOT(K)-1) 43,23,91

```

ORIGINAL PAGE
 OF POOR QUALITY


```

476 43 IF(DABS(T)-DABS(A(I,J,K))) 83,23,23
477 83 IFOW=J
478 ICOL=K
479 T=A(I,J,K)
480 23 CONTINUE
481 9 CONTINUE
482 IPVT(ICOL)=IPVT(ICOL)+1
C FOLLOWING 15 STATEMENTS PUT PIVOT ELEMENT ON DIAGONAL
483 IF(ROW-ICOL) 73,109,73
484 73 DFT=-DFT
485 DO 12 L=1,N
486 T=A(ROW,L)
487 A(ROW,L)=A(ICOL,L)
488 12 A(ICOL,L)=T
489 109 INDEX(I,1)=IPVT
490 INDEX(I,2)=ICOL
491 PIVOT(I)=A(ICOL,ICOL)
492 DFT=DFT-PIVOT(I)
C FOLLOWING 6 STATEMENTS TO DIVIDE PIVOT ROW BY PIVOT ELEMENT
493 A(ICOL,ICOL)=ONE
494 DO 205 L=1,N
495 205 A(ICOL,L)=A(ICOL,L)/PIVOT(I)
C FOLLOWING 10 STATEMENTS TO REDUCE NON-PIVOT ROWS
496 DO 125 LI=1,N
497 IF(LI-ICOL) 21,125,21
498 21 T=A(LI,ICOL)
499 A(LI,ICOL)=ZERO
500 DO 89 L=1,N
501 89 A(LI,L)=A(LI,L)-A(ICOL,L)*T
502 125 CONTINUE
C FOLLOWING 11 STATEMENTS TO INTERCHANGE COLUMNS
503 222 DO 3 I=1,N
504 L=N-I+1
505 IF(INDEX(I,1)-INDEX(L,2)) 19,3,19
506 19 JROW=INDEX(I,1)
507 JCOL=INDEX(L,2)
508 DO 549 K=1,N
509 T=A(K,JROW)
510 A(K,JROW)=A(K,JCOL)
511 A(K,JCOL)=T
512 549 CONTINUE
513 3 CONTINUE
514 81 CONTINUE
C
C SCALE BACK INVERSE OF MATRIX-A
515 DO 2 I=1,N
516 DO 2 J=1,N
517 2 A(I,J)=A(I,J)/SCALE
518 RETURN
C 41 RETURN
519 END

```

//DATA

ERROR INSUFFICIENT MEMORY TO ASSIGN ARRAY STORAGE. JOB ABANDONED

CORE USAGE REJECT CODE= 26312 BYTES,ARRAY APEA= 82752 BYTES,TOTAL APEA AVAILABLE= 104544 BYTES

DIAGNOSTICS NUMBER OF ERRORS= 1, NUMBER OF WARNINGS= 1, NUMBER OF EXTENSIONS= 6

COMPILE TIME= 6.68 SEC, EXECUTION TIME= 0.00 SEC, TAMU/WATFIV - VER 1 LEV 3 JANUARY 1972 DATE= 74/217

APPENDIX B

Tabulation of Wind Tunnel Data

$$S_{REF} = 423.06 \text{ sq. in.}, \quad \bar{c} = 8.36 \text{ in.}$$

1) $q_{\infty} = 50$

LEADING EDGE	STATION NUMBER	VERTICAL DEFLECTION	
		δ_{LE}	δ_{TE}
$\alpha = 2.13$ $C_L = 0.1683$ $C_D = 0.1037$ $C_{PM} = -0.1684$	ON WING		
	3	0.007	-0.015
	4	0.036	-0.015
	5	0.083	0.042
TRAILING EDGE	6	0.176	0.196
	7	0.301	0.239
	8	0.45	0.301
	9	0.584	0.486
	10	0.731	0.682

LEADING EDGE	STATION NUMBER	VERTICAL DEFLECTION	
		δ_{LE}	δ_{TE}
$\alpha = 5.37$ $C_L = 0.461$ $C_D = 0.1215$ $C_{PM} = -0.3301$	ON WING		
	3	-0.029	0.028
	4	0.064	0.079
	5	0.21	0.163
TRAILING EDGE	6	0.442	0.379
	7	0.752	0.662
	8	1.174	0.985
	9	1.617	1.456
	10	2.096	2.005

LEADING EDGE	STATION NUMBER	VERTICAL DEFLECTION	
		δ_{LE}	δ_{TE}
$\alpha = 8.61$	ON WING		
$C_L = 0.758$	3	0.021	0.058
$C_D = 0.1495$	4	0.19	0.163
$C_{PM} = -0.4591$	5	0.442	0.395
TRAILING EDGE	6	0.849	0.71
$\alpha = 8.6$	7	1.406	1.182
$C_L = 0.7521$	8	2.089	1.724
$C_D = 0.1505$	9	2.905	2.491
$C_{PM} = -0.4552$	10	3.742	3.258

II) $q_\infty = 80$

LEADING EDGE	STATION NUMBER	VERTICAL DEFLECTION	
		δ_{LE}	δ_{TE}
$\alpha = 2.13$	ON WING		
$C_L = 0.1676$	3	0.021	-0.22
$C_D = 0.1059$	4	0.064	0.035
$C_{PM} = -0.1671$	5	0.132	0.098
TRAILING EDGE	6	0.282	0.203
$\alpha = 2.13$	7	0.463	0.324
$C_L = 0.167$	8	0.718	0.457
$C_D = 0.1033$	9	0.908	0.747
$C_{PM} = -0.1665$	10	1.175	1.019

LEADING EDGE	STATION NUMBER	VERTICAL DEFLECTION	
		δ_{LE}	δ_{TE}
$\alpha = 5.38$	ON WING		
$C_L = 0.4779$	3	0	0.02
$C_D = 0.1254$	4	0.149	0.155
$C_{PM} = -0.3443$	5	0.408	0.296
TRAILING EDGE	6	0.78	0.535
$\alpha = 5.38$	7	1.323	0.95
$C_L = 0.4759$	8	2.048	1.562
$C_D = 0.1252$	9	2.898	2.286
$C_{PM} = -0.3437$	10	3.678	3.165

LEADING EDGE	STATION NUMBER	VERTICAL DEFLECTION	
		δ_{LE}	δ_{TE}
$\alpha = 8.62$	ON WING		
$C_L = 0.7728$	3	0.048	0.037
$C_D = 0.1540$	4	0.268	0.236
$C_{PM} = -0.4776$	5	0.639	0.591
TRAILING EDGE	6	1.335	1.153
$\alpha = 8.62$	7	2.251	1.891
$C_L = 0.7732$	8	3.356	2.87
$C_D = 0.1503$	9	4.682	4.115
$C_{PM} = -0.4784$	10	6.136	5.505